Growth and mass wasting of volcanic centers in the northern South Sandwich arc, South Atlantic, revealed by new multibeam mapping

Philip T. Leat[a,]*, Alex J. Tate[a], David R. Tappin[b], Simon J. Day[c], Matthew J. Owen[d]

[a]*British Antarctic Survey, High Cross, Madingley Road, Cambridge CB3 0ET, UK*

[b]*British Geological Survey, Kingsley Dunham Centre, Keyworth, Nottingham NG12 5GG, UK*

[c]*Aon Benfield UCL Hazard Research Centre, Department of Earth Sciences, University College London, Gower Street, London, WC1E 6BT, UK*

[d]*Environmental Change Research Centre, Department of Geography, University College London, Gower Street, London, WC1E 6BT, UK*

*Corresponding author. Tel.: +44 1223 221432; Fax.: +44 1223 221646

E-mail Address: ptle@bas.ac.uk (P.T. Leat)

ABSTRACT

New multibeam (swath) bathymetric sonar data acquired using an EM120 system on the RRS *James Clark Ross*, supplemented by sub-bottom profiling, reveals the underwater morphology of a ~12 000 km^2 area in the northern part of the mainly submarine South Sandwich volcanic arc. The new data extend between 55° 45′S and 57° 20′S and include Protector Shoal and the areas around Zavodovski, Visokoi and the Candlemas islands groups. Each of these areas is a discrete volcanic center. The entirely submarine Protector Shoal area, close to the northern limit of the arc, forms a 55 km long east-west-trending seamount chain that is at least partly of silicic composition. The seamounts are comparable to small subaerial stratovolcanoes in size, with volumes up to 83 km^3, indicating that they are the product of multiple eruptions over extended periods. Zavodovski, Visokoi and the Candlemas island group are the summits of three 3-3.5 km high volcanic edifices. The bathymetric data show evidence for relationships between constructional volcanic features, including migrating volcanic centers, structurally controlled constructional ridges, satellite lava flows and domes, and mass wasting of the edifices. Mass wasting takes place mainly by strong erosion at sea level, and dispersal of this material along chutes, probably as turbidity currents and other mass flows that deposit in extensive sediment wave fields. Large scale mass wasting structures include movement of unconsolidated debris in slides, slumps and debris avalanches. Volcanism is migrating westward relative to the underlying plate and major volcanoes are asymmetrical, being steep with abundant recent volcanism on their western flanks, and gently sloping with extinct, eroded volcanic sequences to their east. This is consistent with the calculated rate of subduction erosion of the fore-arc.

Key words: South Sandwich Islands, island arc, submarine volcano, sediment wave, multibeam bathymetry, sub bottom profiling

1. Introduction

Recent studies using multibeam seafloor mapping have added substantial knowledge of the distributions, structures and evolutions of volcanic edifices in intra-oceanic arcs such as the Lesser Antilles arc (Deplus et al., 2001; Le Friant et al., 2004), Izu-Bonin arc (Fiske et al., 2001; Tani et al., 2008), Tonga-Kermadec arc (Wright et al., 2006; Massoth et al., 2007; Chadwick et al., 2008; Graham et al., 2008) and Mariana arc (Oakley et al., 2009). These studies have revealed considerable variability in submarine flank morphology of the volcanoes of intra-oceanic arcs, indicating that they are modified by a range of mass-wasting processes. These range from debris avalanches generated during catastrophic sector collapse (Siebert, 1984; Siebert et al., 1987), to slumps of more coherent material on submarine slopes (Wright et al., 2006; Tani et al., 2008), slide scars generated by small-scale sliding (Chadwick et al., 2008; Chiocci et al., 2008a, 2008b), and flow of volcanigenic sediment away from subaerial zones as turbidity currents. However, the variation in relative importance of these processes in relation to volcano structure, composition, degree of emergence and associated factors such as rates of subaerial and coastal erosion is poorly known.

The intra-oceanic South Sandwich arc, situated in the South Atlantic, consists of large submarine volcanic edifices whose summit form relatively small volcanic islands. Many of the islands are glaciated, and all have high energy erosional coastlines.

Volcaniclastic debris generation in the South Sandwich arc may be a maximum for an intra-oceanic arc, and may be used to contrast arc volcanoes in low-energy ocean environments such as the Bismarck arc (Silver et al., 2009) and Aeolian arc (Favalli et al., 2005) . In this paper, we describe newly-acquired multibeam images and sub bottom profile data of the sea floor around the intra-oceanic South Sandwich arc, and use the data to interpret how constructional and erosional processes interact in this island group.

2. Geological framework of the South Sandwich arc

The volcanically active South Sandwich arc is built on the small oceanic Sandwich plate (Baker, 1990; Barker, 1995; Larter et al., 2003; Leat et al., 2003), and comprises seven main subaerial volcanoes, from Zavodovski in the north to Southern Thule in the south, which form a convex volcanic front (Fig. 1). These subaerial volcanoes are emergent summits of volcanic edifices that rise some 3 km from the Sandwich plate basement. In addition, there is one smaller rear-arc volcanic island (Leskov), and large seamount groups at both ends of the arc (Protector Shoal in the north, and Nelson and Kemp seamounts in the south (Baker, 1990; Leat et al., 2004). The arc is forming in response to steeply inclined subduction of the South American plate beneath the Sandwich plate at a rate of 67-79 mm y^{-1} (Thomas et al., 2003). To the north, the South American plate is tearing in order to subduct, generating a major zone of seismicity (Forsyth, 1975). The associated trench, some 7 km deep, has no significant accretionary complex with virtually all sediment arriving at the trench being subducted (Vanneste and Larter, 2002).

The arc is built on ocean crust formed to the west at the currently active East Scotia Ridge back-arc spreading center (Livermore et al., 1997; Fretzdorff et al., 2002; Livermore, 2003). Magnetic data suggest that the crest of the arc overlies ocean crust of anomaly 5 (9.7-10.9 Ma) in the center of the arc (Larter et al., 2003). To the west of the spreading center, magnetic lineaments can be traced back to anomaly 5B (15.0 Ma). These relationships have been used to suggest that fore-arc has been removed by subduction erosion at a rate of 5.3 km Ma^{-1} over the last 15 Ma (Vanneste and Larter, 2002; Larter et al., 2003).

2.1. Previous bathymetric and geophysical investigations

Seismic data demonstrate the simple crustal structure of the southern South Sandwich arc and fore-arc (Larter et al., 1998, 2003; Vanneste et al., 2002). Smellie et al. (1998) described single beam bathymetric data revealing a ~4.5 km diameter, ~630 m deep caldera between Thule and Cook islands in Southern Thule. This caldera was re-surveyed using multibeam bathymetry in 2006 (Allen and Smellie, 2008). The back-arc East Scotia Ridge and part of the northern fore-arc were mapped in 1995 using towed Hawaii MR1 sonar (Fig. 1b) (Livermore et al., 1997; Vanneste and Larter, 2002; Livermore, 2003).

2.2. South Sandwich Island volcanism and erosion processes

The subaerial parts of the South Sandwich arc volcanoes are relatively well known, following surveys in 1964 (Holdgate and Baker, 1979; Tomblin, 1979) and 1997 (Smellie et al., 1998; Leat et al., 2003). The islands are dominantly basaltic, with dacites and andesites being locally important, and the islands belonging to low-K tholeiitic, tholeiitic, and calc-alkaline magmatic lineages (Pearce et al., 1995, Leat et al., 2003, 2004) Most volcanoes show evidence of recent activity, notably the well-documented eruptions on Bristol Island (1956), Protector Shoal (1962), Saunders Island (1995-1998) and Montagu Island (2001-2004) (Gass et al., 1963; Baker, 1990; Lachlan-Cope et al., 2001; Leat et al., 2003; Patrick et al., 2005).

Onshore investigations show the islands are undergoing very rapid erosion, dominantly coastal. Most of the volcano coastlines are vertical cliffs up to about 350 m in height that are subjected to year-round pounding by Southern Ocean swell. The islands consist of easily eroded sequences of lava, scoria, and ash deposits (Holdgate and Baker, 1979; Baker, 1990; Smellie et al., 1998). Most islands have rugged topography, and several rise to over 400 m high (the highest is 1372 m), despite typically being less than 6 km across. They are devoid of stabilising vegetation, the largest masses of vegetation consisting of moss banks around fumaroles (Longton and Holdgate, 1979; Convey et al., 2000). Most islands, and all of the larger ones, are glaciated, with the glaciers directly entering the sea at ice cliffs. Permanent streams are absent. Where beaches occur, they are extremely high-energy environments, and characterised by large, highly rounded boulders. Significant flat areas occur only on Candlemas Island, where a central area protected by volcanic sequences to either side and connecting boulder beaches has generated a 2x1 km area of trapped sediment (Tomblin, 1979; Leat et al., 2003). These factors suggest that physical erosion rates of the South Sandwich Islands may be maxima for intra-oceanic arcs, with consequently high rates of transport of volcaniclastic sediment down volcano flanks.

3. Methodology

Multibeam data were acquired during in April and May 2007, using a hull-mounted Simrad EM 120 multibeam bathymetric sonar aboard the British research ship RRS *James Clark Ross* (BAS Cruise ID JR168, NERC Cruise leg JR20070418) (Tate and Leat, 2007). The system has a 12 kHz operating frequency and a 191 beam array with real-time beam steering and active pitch and roll compensation. Data were acquired using Simrad's Merlin software and were processed manually using MB System v5.0.9 software. Cleaned data were gridded at 100 m resolution and data were also displayed as a Triangulated Irregular Network to show full resolution surfaces. Vertical measurement accuracy (Simrad specifications) is in the order of 50 cm or 0.2% of depth root mean square (RMS) (whichever is greater). Horizontal resolution varied according to ship speed, water depth, beam angle, track overlap and bottom topography, but is typically 10-20 m at 1000 m and 50-100 m at over 3000 m.

Sub-bottom data were collected using a hull-mounted Simrad TOPAS PS 018 profiler on RRS *James Clark Ross* during (BAS Cruise ID JR206, NERC Cruise leg JR20100118) in January and February 2010. Three lines were run over Seamount PS4 with a combined length of 76.6 km and four separate TOPAS sub-bottom profiler lines with a combined length of 103 km were acquired east of Zavodoski Island. All runs were made using chirp mode on 90% power with a pulse length of 15 ms and start and stop frequencies of 1.5 and 5.0 kHz respectively. Vessel speed varied between 6 and 11 knots, and ping interval was 1500 or 2000 ms, except for line JR206_a (5000 ms). Interpretation of TOPAS data in this area is complicated by limited sediment penetration, and determining whether the lower limit of surficial sediments is a result of signal dissipation or a real boundary between two sediment units is difficult. In the absence of clear lower reflectors, or a sharp change in reflectivity characteristics, we interpret imaged lower boundaries of the surficial units as due to signal dissipation.

The new bathymetric data are shown in Fig. 2A, and Fig. 2B shows derived slopes. The data show for the first time that the submerged parts of Zavodovski, Vioskoi and Candlemas form three distinct edifices. There are no imaged satellite seamounts between these large volcanoes, although small volcanoes occur on the lower flanks of the volcanoes as discussed below. The submarine slopes of the volcanoes are defined by ridges separating wide embayments, narrow chutes descending from shallow shelves and interpreted foci of sediment transport, and steep-sided canyons, occupying lower slopes. The Protector Shoal area in the north is different, consisting of a roughly east-west group of seamounts.

4. South Sandwich arc (55°45' - 57°20')

4.1. Protector Shoal

The entirely submarine Protector Shoal area lies close to the northern limit of the arc. It is thought to have been the source of the eruption which produced an extensive pumice raft that was encountered in the vicinity of Zavodovski Island in March 1962 (Gass et al., 1963), and which subsequently dispersed around Antarctica on the Antarctic Circumpolar Current (Risso et al., 2002). Based on the dimensions of the pumice raft, the volume of pumice produced by this eruption is interpreted to have been at least 0.6 km^3 (Gass et al., 1963). Geochemically, the 1962 pumice is low-K tholeiitic andesite, dacite and (dominantly) rhyolite. Dredge DR.162, recovered during RRS *James Clark Ross* cruise JR18 in 1997 (Leat et al., 2007), from what was then thought to be the southern slope of Protector Shoal, recovered exclusively tholeiitic rhyolite samples which form three distinct compositional groups, that are all different from the 1962 eruption rhyolite. The presence of four distinct silicic magma groups in the pumice and dredged samples led Leat et al. (2007) to propose that the different magmas represented partial melts of distinct mafic sources in the arc crust.

The new bathymetric data (Fig. 3) confirm that the Protector Shoal area is a distinct east-west-trending seamount chain, rather than a single edifice. The chain is some 55 km long, and consists of seven main seamounts, herein called seamounts PS1-PS7, that coalesce to form an underlying east-west trending ridge. None of these edifices corresponds exactly to the location of Protector Shoal as shown on the Admiralty chart (Hydrographic Office, 1989), which shows a 27 m deep summit some 7 km southwest of PS4. PS4 is the closest to Protector Shoal marked on the chart, as well as being the shallowest edifice in the seamount chain, at 55 m deep, and we suggest that PS4 should be recognised as Protector Shoal.

To the north of the seamounts, a distinct faulted terrain is imaged, consisting of north east-southwest-trending faults that downthrow consistently to the southeast and form scarps up to 50 m high (Fig. 3). The faults are interpreted to be related to the flexure of the north edge of the Sandwich plate adjacent to the trench.

Morphological characteristics of the seamounts are summarized in Table 1. They are generally conical and have dome-like summits and smooth flanks. Flank slopes are typically 2-14º, although locally steeper. The seamounts rise some 400-1400 m above their surroundings, and the shallowest (PS4) is only 55 m below sea level. They are clearly constructional volcanic forms. Only seamount PS4 has been sampled (Fig. 3) on its southern flank west of the prominent scar-like structure. Compositions of the other seamounts are unknown, but we suggest that they are also likely to be silicic since they are morphologically similar to PS4. The basal diameters chosen (Table 1) are the isobaths where the seamounts become distinct features, and are probable minima, as they ignore the volume of the underlying ridge-like structure where seamounts coalesce. Calculated volumes range between 4 km^3 for the minor PS3 structure and 55 km^3 and 83 km^3 for PS5 and PS6, respectively. These larger volumes are greater than those of monogenetic rhyolite domes suggesting that the seamounts are composite stratovolcanoes.

The three eastern seamounts PS1, PS2 and PS3 have smooth surfaces with no obvious recently formed features, and are interpreted to be older.

Seamount PS4 has two large flank scars with surface undulations within the scars. The best-preserved scar (Fig. 4A) extends from a south-facing bowl about 2.5 km in width at the summit to the southern base of the seamount. Within the feature, there are a series of well-defined steps, each of which extends across its whole width. The steps are mostly 1.5-2.0 km from front to back and approximately 100-340 m high, and are confined within inward facing lateral margins. The overall slope is ca. 6° in the upper section, reducing to 4° or less on the lower slope. The upper steps slope backward, with well-defined hollows on each step, whereas lower steps become less distinct down-slope. This topography extends for a distance of about 19 km to beyond the base of the seamount, below 2000 m, where it widens to about 10 km. The terrain covers an area of at least 150 km^2. The feature is interpreted as a slump because of its clearly defined source within the south-facing bowl, its well-defined inward facing lateral margins and back-rotated steps.

The down-slope TOPAS line JR206_24 (Fig. 5B) also shows the down-slope gradation, with larger, clearly back-sloping steps in its upper part, and lower relief undulations with no clear evidence for back-rotation on the lower slope. The cross-slope TOPAS line JR206_25 (Fig. 5C) images the 190 m high, inward-facing margins of the slump and its undulating surface, which contrasts to the regular slopes either side of the deposit.

The second scar on the northwest slope of seamount PS4 is smaller, some 4 km in width, and less well-defined. It has similar ca. 100 m high, 0.9 to 1.4 km wide step-like features, imaged by TOPAS (Fig. 5A), to those in the scar on the south flank. The steps slope backward, with well-defined hollows observed on some steps. This feature also is interpreted as a slump. Its inward-facing margins are indistinct, and a channel is interpreted to cut through its lower northern margin forming the low topography north of the slump blocks that is visible in the TOPAS image (Fig. 5A).

Seamount PS5 locally has a bumpy surface, with variable slopes, particularly to the south of the summit (Fig. 3). This may indicate recent lava eruptions. There are several small dome-shaped features notably to the south of the seamount. These are generally some 1-2 km in basal diameter, with heights between 150 and 280 m, giving volumes of about 0.1 to 0.3 km^3, and are probably minor monogenetic satellite lava domes.

Seamount PS6 has the largest calculated volume of 83 km^3 (Table 1). Like PS5, it has a bumpy summit area, probably representing recent lava eruptions, and has a distinct scar on its southwest flank. The latter is about 1.8 km wide, narrower than those on PS4, is straight, and about 13 km long. The upper, steep part of the scar is smooth and featureless, but the lower part is characterized by five step-like features. These are about 1.3 km apart and 100-200 m high, some forming hollows between steps.

Seamount PS7 is ca. 646 m high, appears to surmount a ridge that trends northwest from PS6, and is surmounted by a nested crater complex (Fig. 4B). A 3 km diameter x 140 m deep caldera is cut by a second caldera that is 1.6 km across and 200 m deep. This caldera is clearly breached to the southwest.

4.2. Zavodovski

The new data show that Zavodovski is a locally extensively dissected central volcano that is some 54 km across above the 1800 m isobath (Fig. 6), and the largest volcano in the northern part of the South Sandwich arc. The volcano comprises an eastern and a western ridge, which, although they merge, are interpreted as distinct structures due to differences in morphology as discussed below. The island is situated on the western ridge. None of the submarine features of Zavodovski volcano have been named previously and we use the informal names ZE1-3 and ZW1-6 for constructs on the eastern and western ridges, respectively.

4.2.1 Subaerial edifice, shallow shelf and Mount Curry collapse

Zavodovski Island (Fig. 7A) is about 5 km across and is dominated by a single volcanic cone, Mount Curry (551 m) (Holdgate and Baker, 1979; Baker, 1990). The island has a permanent snowfield, but no significant glaciers. The cone consists of scoria and ash and has a recently active central crater and a second crater to the north which is filled, apparently by material ejected from the active crater (Fig. 7B). Available analyses (Pearce et al., 1995; Leat et al., 2003) indicate that the subaerial products of Zavodovski Island are entirely basalt and basaltic andesite. The active crater and western flanks of Mount Curry are vigorously fumarolically active, a feature of the island noted since the first landings were made during Bellingshausen's expedition in 1819 (Barr, 2000).

Zavodovski Island is surrounded by a shallow shelf to its north, east and south, which is relatively flat and featureless, and mostly between 160 m and 70 m below sea level. The shelf is widest to the southeast of the island, where it is 6 km wide. The shelf appears to continue at about the same depth on the summits of ZE1, ZE2 and ZE3.

*There is southwest-facing embayment i*n ca. 100 m high coastal cliffs, exposing sub-horizontal lavas overlain by scoria and ash deposits apparently interbedded with ice layers (Fig. 7A). We interpret this structure as the head wall of a collapse structure that translated material to the west, herein called the Mount Curry collapse. The subaerial collapse scar is aligned with structures showing evidence for submarine collapse. The adjacent part of the shallow shelf is absent (Fig. 7C), the sea floor lying about 300-400 m below sea level just 2.7 km from the island. This area of lower topography is surrounded by 200 m high inward-facing slopes, forming an embayment some 6.5 km across. The floor of the embayment is very irregular, with a 90 m high hummock in its center (H1 in Fig. 6). Hummock H1 may represent a large translated block. To the west, the collapse feature appears to continue in the form of two sharply defined scars which extend from 500 to 1700 m depth. West of these scars, indistinct hummocky topography occurs to the edge of the survey area, a distance up to 30 km from the island, which may be the associated debris avalanche deposit.

4.2.2. Western ridge

ZW1 is a rugged promontory standing some 200 m high and is 4 km across and may represent an eroded, resistant volcanic center. ZW2 is a 12 km long ridge that extends northwest from the main edifice and shows evidence of a possible landslip scar on its northern flank. ZW2 is interpreted as a constructional volcanic feature, mirroring feature ZW5. Feature ZW3 is a ca. 4 km wide ridge that extends north from Zavodovski Island. At about the 400 m isobath east of ZW2, two subdued embayments are tentatively interpreted as collapse headwalls.

ZW4 is a buttress directly south of Zavodovski Island that has a sub-horizontal surface at about 600 m depth, and is flanked to the east, west and south by slopes up to 20°. The origin of ZW4 is uncertain, but it probably is a constructional feature. An embayment east of ZW4 is interpreted as the head wall of a slump. The lower slopes of the interpreted slump deposit are characterized by arcuate, roughly east-west trending steps with wavelengths of about 1.8 km, possibly masked by later deposits. The relatively gentle slopes at depths between 600 m and 1700 m around ZW5 are characterized by indistinct backward-rotated steps or waves with wavelengths of 1.2-2.0 km, interpreted as slumps or small sediment wave fields. ZW5 is a cone-shaped feature interpreted as a volcanic dome or cone.

ZW6 is a prominent northeast-southwest trending ridge that extends to Leskov Island. The ridge has steep (9-16°), regular slopes that show no apparent evidence of collapse. The feature rises to a flat top at about 640-570 m depth at 28° 50'W, buttressed by a conical form with 10-16° slopes rising to 458 m depth to the southwest. ZW6 is interpreted as a constructional volcanic feature forming a northeast-southwest-trending volcanic ridge joining Zavodovski and Leskov islands.

4.2.3. Eastern ridge

Contructs ZE1-3 form the eastern ridge of the volcano. ZE1 is a prominent flat-topped buttress. Its plateau is 4.4 km across from east to west and mostly 130-140 m below sea level and appears to be smooth and featureless. The sides of ZE1 slope at mostly 5º-12º and have subdued ridges that mostly trend toward the east and northeast. Feature ZE2 is an east-west trending ridge that rises to 140 m below sea level. The south side of this ridge is particularly steep (up to 13º). Feature ZE3 is an approximately circular, nearly flat-topped plateau at 180-120 m depth. There are a series of northeast-southwest trending ridges and troughs with amplitudes of up to 40 m on the plateau. Apart from the narrow 187 m depth ridge that joins it to the Zavodovski shallow shelf, the plateau is flanked by slopes of typically 10°.

Regions to the northwest of ZE1 and between ZE1, ZE2 and ZE3 are occupied by chutes that are approximately 5-7 km wide, with the most prominent being between features ZE2 and ZE3. This chute slopes at an average of about 2º to the east and has a prominent ca. 100 m high central ridge. The chutes have irregularly undulating surfaces consisting of many steps each about 70 m high which modify to progressively more regular wave-like structures with increasing distance from the volcano (Fig. 7D). The step-like features also occur on the northern flank of feature ZE1 and locally on the southern flank of ZE3. The terrain is best developed on the northern flank of ZE1, where the individual steps can be traced for ca. 4 km, and the steps are usually seen to pinch out laterally. The steps have regular dips within each locality.

The origin of features ZE1, ZE2 and ZE3 is uncertain, but similarities suggest a common origin. The chutes that separate them appear to be erosional, dissecting earlier structures. We interpret the features as remnants of an old, extinct part of Zavodovski volcano.

A terrain with distinctive wave-like morphology lies east of Zavodovski volcano. (Fig. 7D). This terrain is about 42 km long in an east-west direction, and extends to the eastern limit of the surveyed area (Fig. 6). It is 40 km in the north-south direction, covering an area of at least 1 200 km^2. The underlying slope is about 2-3°. The terrain is interpreted as a sediment wave field (Section 5.4.6). North of 56º 20'S, a distinct fan has waves strongly parallel to contours and individually traceable over distances up to 14 km. South of that latitude, another fan has waves that are narrower, more sinuous, less parallel to contours and individually traceable up to 10 km. The two fans are separated by a 3 km wide channel that trends east from the chute between ZE2 and ZE3, becomes indistinct below the 1500 m isobath (Fig. 7D), and terminates north of a 350 m high hill (H2, Fig. 6) which appears to be a plug-like feature.

TOPAS sub-bottom imagery across the northern fan (line 27, Fig. 8) shows a gently concave slope with three groups of waves. A group occupying the upper part of the line is heterogeneous, and with wavelengths of about 1.5 km. A central group of large, regular waves have generally flat tops, steep faces, wavelengths of 2.0-3.2 km and amplitudes of 53-149 m. The lower group is again heterogeneous, with wavelengths of 1.0-3.1 km and amplitudes of 65-90 m. The southern fan (line 29, Fig. 8) is more concave with a similar progression of wave size down-slope, although at a generally lower wavelength and amplitude (1.6-2.2 km and 50-105 m in the central section respectively). TOPAS data reveal that the central and lower groups have an upper unit of stratified sediments of typically 20 ms two-way travel time (TWTT) thickness. Assuming a sound velocity through sediments of 1650 m s^{-1} this equates to a thickness of 16.5 m. This unit is locally observed to prograde down-slope from wave crests (Figs. 8A, D) and can be traced from crest to crest on the lower slopes (Figs. A, C), indicating initial formation of the waves as sedimentary bedforms. Occasional deeper reflectors are observed within scarp slopes at depths of up to 30 ms TWTT, equating to a distance of 24.8 m. Somewhat less frequently a deeper unit, characterised by a sharp change in reflectivity, is observed away from the margins of the scarp slopes and below the upper stratified unit (Figs. 8A, D, E) this is interpreted as the boundary between less consolidated upper sediments and more consolidated deeper sediments. We propose that the structures revealed by this boundary, between less and more consolidated sediments, provide evidence of slumped material and faulting or fracturing of sediments. Mounds at the base of steeper slopes (Fig. 8B) and apparently tilted blocks (Fig. 8E) are further evidence for such deformation after initial deposition of the sediment waves.

Zavodovski volcano as a whole is asymmetrical, having significantly steeper slopes to the west than east. The western ridge is dominated by primary volcanic constructs, while the eastern ridge is consists of eroded volcanics and is heavily sedimented. These relationships are consistent with migration of volcanism to the west.

4.3. Visokoi

Visokoi Island is approximately oval in shape, elongated in an E-W direction and about 8 km x 6 km in size (E-W and N-S respectively). It is formed by a single stratovolcano that rises steeply from coastal cliffs to about 1005 m at the summit forming Mount Hodson (Holdgate and Baker, 1979; Baker, 1990; Fig. 9A). Most of the island is currently glacier-covered. The summit is plateau-like, perhaps a crater filled by ice. Around the western sector of the island, the coast consists of high (up to 400-500 m) cliffs that expose successions of interbedded lavas and scoria (Fig. 9B). The eastern sector island cliffs are less than about 100 m high. There is a distinct asymmetry to the island, with slopes to the east of the summit being about half those to the west. A recent lava flow forms a terrace at sea level at the northern point of the island (Holdgate and Baker, 1979), but no unequivocal historical volcanic activity is recorded. According to existing data, volcanic compositions are restricted to basalt and basaltic andesite (Pearce et al., 1995; Leat et al., 2003).

Multibeam data show that Visokoi volcano is a well-defined edifice with dimensions of 40 by 33 km above the 1800 m isobath in east-west and north-south directions respectively (Fig. 10). As with Zavodovski, the island is situated to the west of the edifice center. A well-developed shelf, 2.3 to 6 km wide and shallower than 200 m, surrounds most of the island. The shelf appears to be absent from the southern coast, where water depths reach 300 m within 2 km of the coast, and where the coastal cliffs are notably high. There are no major satellite volcanoes to Visokoi.

Most of the submerged north, west and south slopes of Visokoi are steep (generally in the range 5-12°) and have a characteristic rugged topography producing a large number of small topographic highs (Fig. 9C). These highs are up to 2 km across and up to about 350 m above the surrounding slopes. Many have approximately conical shapes, steep down-slope scarps (clearly seen on the slope plot, Fig. 2B). This topography occurs down to 2400 m water depth and up to 11 km from Visokoi Island, especially to the southwest. We interpret this topography as formed by eruption of domes or cones and effusion of lavas. Similar terrains have been imaged in submarine volcanic rift zones and on relatively stable submarine volcano flanks in Hawaii and the Canary Islands (Mitchell et al., 2002; Eakins and Robinson, 2006). The terrain is cut by chutes west of the island and down-slope of the terrain there is a heterogeneous terrain characterised by random distribution of hummocks up to about 100 m high, interpreted as debris that has slid down the chutes from the eruption sites (Fig. 10).

The east flank of Visokoi volcano is different. It forms a smooth, featureless plateau that is 15 km wide in an east-west direction and some 17 km across in a north-south direction (Fig. 10). The plateau slopes gently east from a depth of less than 200 m to ca. 600 m 12 km from the volcano. To the east the plateau passes into an area of deep canyons which may be a northward extension of a prominent structure which we informally name Ridge A.

The main segment of Ridge A is a curved, approximately NNW-SSE-trending positive feature connecting the Visokoi and Candlemas edifices (Fig. 10). It is about 30 km long and rises some 600-1000 m above the surrounding topography. The summit area of the ridge is gently undulating and rises toward both Visokoi and Candlemas, with a central saddle at 980 m depth. Its western flank is relatively featureless and has slopes of generally 3-8°. In contrast, its eastern flank is cut by several main canyons, each with distinct headwalls and gullies that trend toward the northeast, and each separated from adjacent canyons by ridges 200-600 m high and up to 20 km long. Canyon headwall and sidewall slopes are typically about 10° and locally up to 24°. There are no obvious hummocky deposits on the floor of the canyons. They are interpreted as erosional forms generated by mass wasting to the northeast. Interestingly, all the canyons have floors around 1600-1800 m deep, suggesting that erosion is likely occurring down to a lithologically controlled level.

Visokoi volcano as a whole, like Zavodovski, is asymmetrical, with young volcanism forming steep slopes to the west, and eroded terrains to the east.

4.4. Candlemas Group

The two main islands of the group, Candlemas and Vindication islands are 4.5 km apart. The larger, 6 by 4 km Candlemas Island (Fig. 11A) consists of an older, lava-dominated series that forms the glacier-covered south of the island, and a recently-erupted group of lavas and scoria cones including the 232 m high Lucifer Hill that form the north of the island (Holdgate and Baker, 1979, Tomblin, 1979; Leat et al., 2003). The older sequence rises to 550 m at Mount Andromeda (Fig. 11B). Dips of bedding in the sequence are variable and do not match topography, indicating that the sequence is strongly eroded. Local dips indicate the presence of several centers. For example dips to the southwest on Mount Perseus indicate a former eruption center northeast of the island. Vindication Island (1.5 x 3 km) consists of a similar lava sequence rising to 426 m at Quadrant Peak (Fig. 11C). The island group is compositionally bimodal, with basalts and basaltic andesites forming the older series on both Candlemas and Vindication, and andesites and dacites forming the younger Lucifer Hill lavas (Leat et al., 2003). The recent cone and associated blocky lava flows of the Lucifer Hill volcanic center are separated from the older series of Candlemas Island by boulder and shingle spits and lagoons (Figs. 11D, E). The recent lavas are interpreted to form lava deltas with a radius of ca. 1 km from the cone. There is no historical record of witnessed volcanic eruptions, but Lucifer Hill is strongly fumarolic. The boulder and shingle spits likely accumulated in the lee of the Lucifer Hill center, implying rapid sediment accumulation since the growth of that volcano.

The submerged Candlemas edifice is approximately circular in plan, with a diameter of about 32 km above the 1800 m isobath (Fig.10). The submerged flanks slope steeply away from the islands on all sides, except to the north where the volcano merges with Ridge A. According to soundings (Hydrographic Office, 1989), an extensive shallow shelf mostly less than 100 m in depth and about 12 km in diameter occupies most of the unsurveyed area close to the islands (Fig. 11A). There are numerous small islands, sea stacks and shoals on the shelf, such as Tomblin Rock, Santa Rock and Cook Rock that are interpreted as eroded remnants of formerly more extensive subaerial volcanoes. The shelf is much less extended southeast and south of Candlemas Island, but extends 5 km to the north and northwest of Candlemas and Vindication islands. None of the submarine features around the Candlemas island group has been named and we use the informal names CA1-5 to identify the major positive features and ECE, SCE, WCE and NCE to identify prominent embayments.

There is no strong E-W contrast in edifice structure and features are described clockwise from the north.

Ridge CA1 forms the north flank of a 16 km wide east-facing embayment that we name the East Candlemas Embayment (ECE), and that appears to consist of two parts (ECE1 and ECE 2, Fig. 10). CA1 has a steep (up to 24°), 12 km long south-facing slope that contrasts with its more gently sloping north-facing slope. The steep southern slope of CA1 may be a collapse scar sidewall, suggesting that ECE is a large, perhaps composite, collapse feature. CA2 forms the southern flank of ECE and is relatively featureless with a steepened north-facing slope. The northern, central part of the embayment, ECE1, is ca. 12 km wide, generally smooth below 1000 m depth, and is formed of coalescing minor landslide scars or chutes above that depth. The southern part of the embayment, ECE2, is formed by a ca. 100 m deep, ca. 3.5 km wide trough that appears to be superimposed on and younger than ECE1. To the east of ECE2, below 2000 m there is indistinct hummocky topography, and ECE2 is interpreted as the more recently active chute for sediment mass movement.

Between CA2 and CA3, the South Candlemas Embayment (SCE) consists of three small embayments 1.7 to 3 km in width that are separated by ridges. The head walls of all three small embayments terminate at approximately 600 m depth. All are interpreted to be landslide scars, and are also probably chutes funnelling sediment away from the shelf. To the southeast of these embayments, topography is dominated by contour-parallel wave-like features on an underlying slope of 2-5°. The waves are branching, generally 1.4- 1.8 km wide and 50-150 m high, with their tops sloping back toward the volcano, forming distinct hollows. This terrain is interpreted as a sediment wave field, possibly modified by slumping, formed by sediment discharging from the three small embayments.

CA3 and CA4 are relatively smooth ridges up to about 400 m high that form spurs extending to the southwest. Their lower slopes consist of rounded terraces which are steep on their downhill margins. These terraces are interpreted as lava flows, and ridges CA3 and CA4 as constructional features.

The west flank of Candlemas consists of the relatively smooth and featureless West Candlemas Embayment WCE (Fig. 10). This embayment occupies about 90° of arc between ridges CA4 and CA5. Above about 700 m the embayment divides into four narrow chutes. The floor of WCE is smooth above about 1600 m, and below that is more uneven. We interpret WCE as a largely constructional apron, probably covered by sediment moving down-slope from the shallow shelf, probably as turbidity currents, although the slopes lack prominent wave-like forms.

CA5 is a smooth ridge that extends northwest from the islands and terminates at a seamount rising to 950 m. CS5 is interpreted as a constructional volcanic ridge with the seamount representing a satellite volcano. The northeast-facing slope of CA5 forms the southwest flank of an asymmetrical embayment (North Candlemas Embayment, NCE in Fig. 10). A prominent 1.5 km across by 150 m high conical hummock (H3 in Fig. 10) is interpreted as a volcanic cone. The floor of NCE south of H3 and between 600 m and 1100 m consist of five step-like features widening to 1.4 km wide at the base interpreted as a 5 km long by 3.5 km wide slump. A prominent scarp follows the 1400 m contour and is marked by a ca. 50 m deep trough below a

200 m high cliff. This appears to be the headwall of a separate, lower slump. The slope between 1400 m and 1900 m is hummocky, with no clear linearity to features, and may represent a debris avalanche deposit or slump. Below 1800 m, on slopes of 1-3º, indistinct contour-parallel sediment waves with wavelengths of about 2.2 km are present.

The Candlemas edifice contrasts with those of Zavodovski and Visokoi in having little east-west asymmetry, although primary constructional forms occur only on its western slopes, and sediment waves are more prominent to the east.

5. Discussion

The newly acquired data show a range of volcanic morphology formed by both constructional and erosional processes.

5.1. Size and profiles of the volcanoes

The size of the Protector Shoal seamounts (Table 1) may be compared to volcanoes of the Tonga-Kermadec arc (Wright et al., 2006; Massoth et al., 2007), which is also a dominantly submarine, intra-oceanic arc. Volumes of individual Protector Shoal seamounts, 9-83 km^3 (excepting PS3) are similar to Tonga-Kermadec stratovolcanoes and silicic caldera volcanoes (15-269 km^3) (Wright et al., 2006). The Protector Shoal seamounts are also comparable in size to the smaller individual eruptive centers in subaerial arc volcanoes, such as South Soufrière Hills-Soufrière Hills dome complex on Montserrat which has a current subaerial volume of 12 km^3 and an estimated total subaerially erupted volume of 30 km^3 (Le Friant et al., 2004). The nested caldera complex PS7 is unique in the Protector Shoal area, but nested or multiple calderas of similar dimensions (Volcano 16, Volcano 19, Sonne volcano; Hinetapeka volcano, Putoto volcanic center) are common in the Tonga-Kermadec arc (Wright et al., 2006; Massoth et al., 2007; Graham et al., 2008). The strong association of submarine stratovolcanoes and silicic calderas with hydrothermal activity and polymetalic sulphide deposits in the Tonga-Kermadec (de Ronde et al., 2001; Baker et al., 2003; Massoth et al., 2007) and Mariana and Izu-Bonin (Stüben et al., 1992; Iizasa et al., 1999; Fiske et al., 2001) arcs suggests that the Protector Shoal seamounts may be likely sites for hydrothermal venting. As caldera structures and associated faults localize hydrothermal activity, PS7 is a particularly promising vent search target.

The three main volcanoes, Zavodovski, Vioskoi and Candlemas are relatively large stratovolcanoes. east-west profiles indicate that the volcanoes rise, from a base of approximately 2500 m water depth (Fig. 12), to heights above this base of 3000-3500 m. Their basal diameters at the 2500 m level range from >53 km (Candlemas) to 57 km (Visokoi) and 83 km (Zavodovski). Volcano volumes are approximately 2 200 km^3 (Candlemas), 3 000 km^3 (Visokoi) and 5 400 km^3 (Zavodovski). Profiles (Fig. 12) show that all the volcanoes are asymmetrical, having steep western flanks and, overall, relatively gentle eastern flanks. This is consistent with the general erosional character of the eastern flanks of the volcanoes and the presence of young constructional features on their western flanks, and is interpreted to result from migration of active volcanic centers, especially Zavodovski and Visokoi, to the west relative to the underlying plate.

5.2. Shallow Shelves

Shallow shelves occur around Zavodovski Island, the eastern side of Vioskoi, and the area around Candlemas and Vindication islands. There are several possible origins for these shallow shelves: tectonic subsidence of wave-cut platforms, erosion of wave-cut platforms during times of low sea level; emplacement of lava deltas during times of low sea level; erosion along a lithological transition; and iceberg scouring. Similar shallow shelves having similar widths occur on emergent arc volcanoes in many volcanic arcs, including Izu Bonin (Tani et al., 2008), Lesser Antilles (Le Friant et al., 2004), Aeolian (Favalli et al., 2005) and Aleutian (Coombs et al., 2007). The presence of clearly erosional remnants projecting above the surface, most notably the older lava series on Vindication and Candlemas islands and sea stacks such as Cook Rock, is taken to indicate that the shelves are products of erosion and not emplacement of lava deltas. Icebergs derived from Antarctic ice shelves have keel depths of about 140-600 m and are known to scour substrate at these depths (Dowdeswell and Bamber, 2007). Large icebergs, mostly derived from the Ronne-Filchner ice shelf, are continuously present around the South Sandwich Islands and commonly become grounded on the shallow shelves close to the islands. Although iceberg scouring must affect the shallow shelves, it is not thought to have formed them, because shallow shelves are clearly a global phenomenon, and not restricted to the reach of icebergs. There is no evidence that the shallow shelves represent erosion along a lithological boundary. An increase in explosive generation of (easily eroded) fragmentary deposits during the growth of a submarine volcano is likely, as eruption sites become shallower. This is not likely to form a well-defined boundary at <200 m, but more likely to be a gradual transition in explosive and fragmentation processes over a large and deeper range (Kokelaar, 1986; Head and Wilson, 2003). Le Friant et al. (2004) showed that the width of shallow shelf increased with increasing age of volcanism at Montserrat, Lesser Antilles. This is strong evidence that the Montserrat shelves formed by erosion at sea level during glacially controlled low stands, and not by tectonic subsedence. We follow this reasoning and interpret the South Sandwich shallow shelves as wave-cut platforms formed during low sea level stands.

5.3. Primary constructional volcanic features

Primary constructional volcanic features are identified as being amundant in the survey area. The seamounts of the Protector Shoal area are dominantly constructional, with smooth slopes interpreted as tephra and volcaniclastic deposits draped over locally more bumpy lava terrain. There are small, ca. 1-2 km diameter satellite domes around the larger volcanoes. The rugged topography of the submerged north, west and south slopes of Visokoi is interpreted as constructional, with numerous domes, cones or lavas up to 2 km in diameter.

Several ridges on Zavodovski and Candlemas are interpreted as primary constructional volcanic features. The ridge from ZW5 to ZW6 southwest of Zavodovski is the clearest example. Its steep, rugged slopes do not appear to have been affected by collapse, and the feature rises to a conical summit at 458 m depth, interpreted as a seamount. ZW2 on Zavodovski is interpreted as similar, but smaller, although its northern slope appears to have been modified by sliding. CA3, CA4 and CA5 on Candlemas are interpreted as constructional ridges. CA3 and CA4 are associated with terrace-like topography interpreted as lavas and do not appear to have been modified by collapse. CA5 rises to a conical summit at 950 m depth and is interpreted as a seamount. All these ridges extend linearly either northwest or southeast from the central volcanoes, implying structural control. They are interpreted to be the same as the fissure ridges described from the Kermadec-Tonga arc (Wright et al., 2006; Graham et al., 2008), and are interpreted as formed by eruption from structurally controlled dike systems.

5.4. Mass wasting

There is abundant evidence for extensive mass wasting of the northern South Sandwich arc. Erosional remnants, locally interpreted to expose trap-like volcanic series are widespread and there are many sediment chutes interpreted to channel sediment down volcano flanks. We interpret a large number of collapse structures of several different types from the morphological analysis that clearly indicate that mass movements occurred repeatedly during volcano evolution.

5.4.1 Sediment chutes

Sediment chutes are interpreted to form a radial pattern on Zavodovski, with prominent examples west of ZE1, between ZE1 and ZE3, and west of ZW3. On Candlemas, a radial pattern of chutes is also evident. ECE2 is interpreted as a sediment chute, while WCE, ECE1and SCE embayments are interpreted as broader aprons down which sediment is transported, all of which divide into narrow chutes adjacent to the shallow shelf. All these chutes originate from shallow shelves around islands, suggesting that the shelves are the sediment sources, and that the chutes channel sediment movement down volcano slopes. It some cases, such as the three small embayments in SCE, chutes probably occupy former slide scars. Many of the chutes, especially north and east of Zavodovski and south of Candlemas spatially correlate with sediment wave fields down-slope, indicating sediment movement in the chutes was as turbidity currents or other mass flows. The high rate of sediment supply to the chutes required to feed such flows is consistent with the evidence for high rates of erosion in the coastal zone.

5.4.2. Slide scars

The 13 km long, 1.8 km wide scar on the southwest flank of seamount PS6 is interpreted as a slide scar. The scar has similarities with the Sciara del Fuoco on Stromboli volcano and transient slide scars observed on the cone of Monowai volcano, Kermadec arc. The Sciara del Fuoco collapse scar extends from the subaerial to submarine environment and is the location of repeated sediment transport in events that range from mass failure landslides to small slides and gravity flows (Chiocci et al., 2008a, 2008b; Romagnoli et al., 2009). The PS6 slide scar and Sciara del Fuoco have similar lengths (13-20 km) and widths (ca. 2 km at their proximal ends), but the Sciara del Fuoco is steeper at its proximal end (>30°) than the PS6 scar (ca. 13°). The several, transient, submarine slide scars that developed on Monowai volcano between 1998 and 2007 developed on a smaller cone, and are ca. 4 km long, and were caused by sliding of unstable fragmental material on the steep (>20°) summit and upper slopes of the cone (Chadwick et al., 2008). The PS6 scar is interpreted as a slide scar formed by failure of fragmental material as small slides and gravity flows on its steep upper slopes.

5.4.3. Debris avalanches

The term debris avalanche is used for rapidly-moving, catastrophic failures in which rock masses are transformed into fragmented debris, and whose deposits form hummocky or blocky terrain. These have been reported from submarine parts of many arcs including the Lesser Antilles (Deplus et al., 2001), Aleutians (Coombs et al., 2007), Bismarck arc (Silver et al., 2005, 2009) and Japan Sea (Satake and Kato, 2001).

The Mount Curry collapse feature on Zavodovski (Figs. 7A, C) is interpreted to have formed a debris avalanche. Importantly, the collapse occurred on the steep western side of the volcano. The area (20 km^2) and thickness (0.2 km) of shallow shelf missing in the collapse scar indicates a volume of ca. 4 km^3 for the debris avalanche, which probably occupies the area of indistinct hummocks extending to the edge of the survey area. The entire structure has characteristics of major volcano flank collapses forming large debris avalanches (Siebert, 1984; Siebert et al., 1987; Silver et al., 2005). The volume, vertical drop of about 3.1 km and travel distance of at least 30 km, are consistent with the larger (>1 km^3) debris avalanches associated with volcano sector collapse (Siebert et al., 1987).

The hummocky terrain west of Visokoi below 2300 m is interpreted as probably being debris avalanche deposits. These are interpreted to have been derived from collapse of the steep, constructional western flank of Visokoi, and are associated with two chutes in the steep western flank of Visokoi: any horseshoe scars representing the upper limit of the collapse features might have been buried by later volcano growth. Collapses of similar steep, submarine volcano flanks to form debris avalanches deposited as similar hummocky terrains are found on Hawaii, the Canary Islands and Samoa (Lipman et al., 1988; Keating et al., 2000; Mitchell et al., 2002). The ECE2 scar on Candlemas is a likely debris avalanche collapse feature, with a well-defined chute that has apparently eroded into the large ECE1 embayment, and hummocky topography below

2000 m. Debris avalanche deposits may exist in the NCE on Candlemas, although these deposits cannot be interpreted unequivocally from the multibeam data.

5.4.4. Slumps

Slumps, which used here include collapsed sediments (Keating et al., 2000; Tappin et al., 2001; Tani et al., 2008) that were mostly coherent rather than fragmented, are widespread in the area. The slump on the south flank of seamount PS4 is particularly clear, and interpreted as a slump because of its clearly related source within the south-facing bowl, its confinement within inward-facing lateral walls and back-rotated steps. There is an insufficient sediment source for its steps to be sediment waves generated by sediment transport from the summit of PS4, and an origin as eruption-generated mass flows is unlikely because of its well-defined lateral limits. It has a well-defined gradation of structure with distance from source, with progression from a large upper rotated slump block, to tilted slump blocks (Fig. 5B). In its lower part imaged by TOPAS, evidence for block rotation is lost, and the sediment may have been deposited as a disaggregated mass. It is interpreted to have moved initially as a series of rotated blocks, with deformation concentrated on an underlying slide surface. The progressive variations along the surface, confinement within a single set of inward-facing walls and association with a single source bowl suggest it formed as a single event, rather than repeated failure of the seamount slopes.

Several similar features within the mapped area characterised by step-like components of similar dimensions, often with distinct horseshoe-shaped source areas are also interpreted as slumps, although we cannot interpret whether deformation was by creep or at a high rate. On Zavodovski, slumps with good evidence for head walls, inward-facing lateral walls and deposits that appear to have moved coherently, forming tilted slump blocks, are interpreted to the east of ZW4 and possibly on the northern slope of feature ZW2. In the Candlemas NCE, there are two well-imaged slump structures. The occurrence of the slumps in an area of high seismicity suggests that they were triggered by earthquakes.

5.4.5. Step-like features in eroded terrains

The step-like features that occur on the 5-12° northern flank of feature ZE1, locally on the southern flank of ZE3, and in adjacent chutes are distinctive. They are gently-dipping, about 70 m high, laterally continuous but pinch and swell in height and extend across both chutes and adjacent flanks of positive features (Fig. 6). We interpret these as products of erosion of lava or sill-dominated sequences producing trap-like terrains. Their exposure is interpreted to have resulted from repeated collapse of volcano edifices and scouring by turbidity currents and other mass flows. A similar step-like geomorphological form is apparent on edifice ‘Q’ in the extinct proto-Kermadec arc, which exposes volcanic basement on its steeper flanks (Graham et al., 2008).

5.4.6. Sediment waves

Undulating, wave-like seabed morphologies have several different origins. Sediment waves can form as contourites or from turbidity currents (Damuth, 1979; Migeon et al., 2000). Contourite sediment waves formed by sediment transport and deposition from ocean currents are associated in the Scotia Sea region with the Antarctic Circumpolar Current and northern outflow of Weddell Sea Deep Water (Pudsey, 2002; Cunningham et al., 2002; Maldonado et al., 2003). They have irregular forms and scales, and are controlled by sea floor topography and current directions. Sediment waves deposited from turbidity currents occur on continental margins, flanks of volcanic islands and abyssal trenches (Normark et al., 2002). They form fields of regular, rhythmic waves with axes approximately parallel to contours and are associated with a distinct source region and levee and overbank deposits related to channels which concentrate the turbidity current flow. Waves vary from 2 to ca. 70 m in height, with wavelengths of 0.2 to 5 km and tend to migrate up slope (Damuth, 1979; Migeon et al., 2000; Wynn et al., 2000, 2002; Normark et al., 2002; Lee et al., 2002). Wave-like morphologies also occur due to deformation in slumps and down-slope creep, which may modify sediment waves, as proposed for sediment wave fields associated with the Bismarck volcanic arc (Hoffmann et at., 2010). Concentric ridges may also form from density flows associated with eruptions (Wright et al., 2006).

The sediment wave field that extends from Zavodovski to the east of the survey area (Fig. 7D) is interpreted as formed from turbidity currents rather than as contourites. The evidence for this interpretation is that the waves parallel isobaths, are concentric to the likely sediment source discharging from chutes east of the volcano, and the field has a central channel trending east from the chute between ZE2 and ZE3. The close spatial association of the sediment wave field with the chutes channeling sediment from the shallow shelf indicates that the shelf was the main sediment source, and the alignment of the chute between ZE2 and ZE3 with the central channel suggests this was a major transport route and the component northern and southern fans of the sediment wave field may be interpreted as overbank deposits. The interpretation is consistent with the identification of sediments deposited from turbidity flows in cores from the South Sandwich fore-arc (Howe et al., 2004). The wave field decreases in wavelength and height with distance from source, as expected for sediment waves derived from turbidity currents (Lee et al., 2000). The amplitude of the larger sediment waves is in the upper range for sediment waves derived from turbidity currents, suggesting strong, sediment-laden flows. The comparable, but larger, sediment wave field on the flanks of La Palma, Canary Islands (Wynn et al., 2000), for example, is typified by smaller wavelengths (0.4-2.4 km) and amplitudes (<70 m). Hoffmann et al. (2010) demonstrated that otherwise comparable sediment wave fields associated with volcanoes of the Bismarck arc show different wave asymmetries, which they suggested is a result of variable down-slope deformation of the waves by slumping. The Zavodovski sediment wave fields have heterogeneous, asymmetrical waves in their upper slopes, exposed boundaries between less and more consolidated sediments, mounds at the base of steeper slopes and tilted blocks suggesting that down-slope deformation of the sediment waves as they accumulated was pervasive.

5.5. Migration of volcanoes

The South Sandwich fore-arc is currently being eroded at the trench by subduction erosion at 5.3 km Ma^{-1} (Vanneste and Larter, 2002; Larter et al., 2003). Assuming a constant slab dip, this suggests westward migration of volcanic centers at this rate relative to the underlying plate. Several features of Zavodovski and Visokoi suggest such westerly migration, although Candlemas less so. These are the asymmetrical form of the volcanoes, with steep western and shallow but incised eastern flanks, the occurrence of all the interpreted constructional volcanic forms on the western side of the volcanoes, and the concentration of more eroded and sedimented terrains on their eastern flanks. Zavodovski shows these features well, in the migration of activity from the east ridge to the west ridge with time. East ridge edifices ZE1-3 are interpreted as extinct, eroded volcanic remnants, whereas the west ridge of the volcano, notably ZW2, ZW4, ZW5 and ZW6, are interpreted as constructional features on the same loci of magmatism as the active volcanic island. At the rate of erosion calculated for the fore-arc, if ZE1, ZE2 and ZE3 originally erupted at the volcanic front, they formed about 2-2.6 Ma, and Ridge A about 2-4 Ma.

6. Conclusions

The new multibeam data reveal, for the first time, the main volcanic features of the northern part of the South Sandwich arc, and the mass-wasting process that affected them.

1. The Protector Shoal area consists of seamounts that range from 400 to 1400 m in height, and have volumes up to 83 km^3. PS7 has a 3 km diameter x 140 m deep nested summit caldera. Dredging shows that PS4 is rhyolitic in composition, and the others are suspected of also being dominantly silicic.
2. Zavodovski, Visokoi and Candlemas are three large volcanoes, with heights of 3000-3500 m above surrounding sea floor and complex histories including collapse. The volcanoes are asymmetrical, Zavodovski and Visokoi more so than Candlemas, having steep west flanks and gently sloping east flanks.
3. Zavodovski has an older eastern ridge and a younger western ridge on which the island is situated. The east of the volcano is strongly incised by erosion, with the development of chutes that channel sediment down-slope to be deposited in sediment wave fields. The western ridge is dominated by constructional volcanism, with a prominent fissure-fed ridge extending to the southwest. The western part of the island has collapsed as a debris avalanche.

4. Visokoi has steep slopes on its north, west and south flanks, which have rugged topographies interpreted as resulting from recent lava and dome eruptions. Its east flank joins with a strongly eroded ridge interpreted as representing an earlier phase of magmatism.
5. The Candlemas edifice includes the islands of Vindication and several sea stacks. It has features interpreted as fissure-fed constructional volcanic ridges, separated by sediment-covered embayments affected by slumping.
6. The islands have shallow shelves of variable depth, but mostly less than 160 m, and interpreted as wave-cut platforms eroded during times of low sea level.
7. There is abundant evidence for mass wasting processes affecting the submarine edifices, including landsliding as debris avalanches and slumps. Erosion rates are high, due to glacial and coastal processes, generating large sediment volumes on the shallow shelves. Such sediment is transported, especially to the east, from shallow shelves through chutes to the lower volcano slopes as turbidity currents and other mass flows, generating sediment wave fields. Sediment wave fields appear to be modified by local slumping.
8. Most recent volcanism is generally on the west flanks of the volcanoes, while their east flanks are interpreted as dominated by extinct, eroded features. The volcanoes are interpreted to have migrated to the west relative to the underlying plate, consistent with the rate of subduction erosion of the fore-arc of 5.3 km Ma^{-1} (Larter et al., 2003).

Acknowledgements

This study is part of the British Antarctic Survey Polar Science for Planet Earth Programme. It was funded by The Natural Environment Research Council. We are grateful to Captains Graham Chapman and Jerry Burgan and crews of RRS *James Clark Ross* for their enthusiastic support of the work. The paper greatly benefitted from constructive comments by C. Romagnoli and an anonymous reviewer.

References

Allen, C., Smellie, J.L., 2008. Volcanic features and the hydrological setting of Southern Thule, South Sandwich Islands. Antarctic Science 20, 301-308.

Baker, E.T., Feeley, R.A., de Ronde, C.E.J., Massoth, G.J., Wright, I.C., 2003. Submarine hydrothermal venting on the southern Kermadec volcanic arc front (offshore New Zealand): location and extent of particle plume signatures, in: Larter, R.D., Leat, P.T. (Eds.), Intra-Oceanic Subduction Systems: Tectonic and Magmatic Processes. Geological Society, London, Special Publications 219, pp. 141-161.

Baker, P.E., 1990. South Sandwich Islands, in: LeMasurier, W.E, Thomson, J.W. (Eds.), Volcanoes of the Antarctic Plate and Southern Oceans. Antarctic Research Series, AGU, Washington, D.C., vol. 48, pp. 361-395.

Barker, P.F., 1995. Tectonic framework of the East Scotia, in: Taylor, B. (Ed.) Backarc Basins: Tectonics and Magmatism. Plenum Press, New York, pp. 281-314.

Barr, W., 2000. First Landings on Zavodovski Island, South Sandwich Islands. Polar Record 36, 317-322.

Chadwick, W.W., Wright, I.C., Schwarz-Schamera, U., Hyvernaud, O., Reymond D., de Ronde, C.E.J., 2008. Cyclic eruptions and sector collapses at Monowai submarine volcano, Kermadec arc: 1998-2007. Geochemistry Geophysics Geosystems 9, Q10014, doi:10.1029/2008GC002113.

Chiocci, F.L., Romagnoli, C., Bosman, A., 2008a. Morphological resilience and depositional processes due to the rapid evolution of the submerged Sciara del Fuoco (Stromboli Island) after the December 2002 submarine slide and tsunami. Geomorphology 100, 356-365.

Chiocci, F.L., Romagnoli, C., Tommasi, P., Bosman A., 2008b. The Stromboli 2002 tsunamigenic submarine slide: characteristics and possible failure mechanisms, Journal of Geophysical Research 113, B10102, doi:1029/2007JB005172.

Convey, P., Smith, R.I.L., Hodgson, D.A., Peat, H.J., 2000. The flora of the South Sandwich Islands, with particular reference to the influence of geothermal heating. Journal of Biogeography 27, 1279-1295.

Coombs, M.L., White, S.M., Scholl, D.W., 2007. Massive edifice failure at Aleutian arc volcanoes. Earth and Planetary Science Letters 256, 403-418.

Cunningham, A.P., Howe, J.A., Barker, P.F., 2002. Contourite sedimentation in the Falkland Trough, western south Atlantic, in: Stow, D.A.V., Pudsey, C.J., Howe, J.A., Faugères, J.-C., Viana, A.R. (Eds.), Deep-Water Contourite Systems: Modern Drifts and Ancient Series, Seismic and Sedimentary Characteristics. Geological Society, London, Memoirs 22, pp. 337-352.

Damuth, J.E., 1979. Migrating sediment waves created by turbidity currents in the northern South China Basin. Geology 7, 520-523.

Deplus, C., Le Friant, A., Boudon, G., Komorowski, J.-C., Villemant, B., Harford, C., Ségoufin, J., Cheminée J.-L., 2001. Submarine evidence for large-scale debris avalanches in the Lesser Antilles arc. Earth and Planetary Science Letters 192, 145-157.

de Ronde, C.E.J., Baker, E.T., Massoth, G.J., Lupton, J.E., Wright, I.C., Feeley, R.A., Greene, R.R., 2001. Intra-oceanic subduction-related hydrothermal venting, Kermadec volcanic arc, New Zealand. Earth and Planetary Science Letters 193, 359-369.

Dowdeswell, J.A., Bamber, J.L., 2007. Keel depths of modern Antarctic icebergs and implications for sea-floor scouring in the geological record. Marine Geology 243, 120-131.

Favalli, M., Karátson, D., Muzzuoli, R., Pareschi, M.T., Ventura, G., 2005. Volcanic geomorphology and tectonics of the Aeolian archipelago (southern Italy) based on integrated DEM data. Bulletin of Volcanology 68, 157-170.

Eakins, B.W., Robinson, J.E., 2006. Submarine geology of Hana Ridge and Haleakala Volcano's northeast flank, Maui. Journal of Volcanology and Geothermal Research 151, 229-250.

Fiske, R.S., Naka, J., Iizasa, K., Yuasa, M., Klaus, A., 2001. Submarine silicic caldera at the front of the Izu-Bonin arc, Japan: voluminous seafloor eruptions of rhyolite pumice. Geological Society of America, Bulletin 113, 813-824.

Forsyth, D.W., 1975. Fault plane solutions and tectonics of the South Atlantic and Scotia Sea. Journal of Geophysical Research 80, 1429-1443.

Fretzdorff, S., Devey, C.W., Livermore, R.A., Leat P.T., Stoffers P., 2002. Petrogenesis of the back-arc East Scotia Ridge, South Atlantic Ocean. Journal of Petrology 43, 1435-1467.

Gass, I.G., Harris, P.G., Holdgate, M.W., 1963. Pumice eruption in the area of the South Sandwich Islands. Geological Magazine 100, 321-330.

Graham, I.J., Reyes, A.G., Wright, I.C., Peckett, K.M., Smith, I.E.M., Arculus, R.J., 2008. Structure and petrology of newly discovered volcanic centres in the northern Kermadec-southern Tofua arc, South Pacific Ocean. Journal of Geophysical Research 113, B08S02, doi:10.1029/2007JB005453.

Head, J.W., Wilson, L., 2003. Deep submarine pyroclastic eruptions: theory and predicted landforms and deposits. Journal of Volcanology and Geothermal Research 121, 155-193.

Hoffmann, G., Silver, E., Day, S.J., Driscoll, N. & Orange, D., 2010. Deformation versus deposition of sediment waves in the Bismarck Sea, Papua New Guinea, in: Shipp, R.C., Weimer, P., Posamentier, H.W. (Eds.), Mass Transport Deposits in Deepwater Settings, SEPM (Society for Sedimentary Geology), Tulsa, Special Publications 95 in press.

Holdgate, M.W., Baker, P.E., 1979. The South Sandwich Islands: I. General description. British Antarctic Survey Scientific Reports 91.

Howe, J.A., Shimmield, T.M., Diaz, R., 2004. Deep-water sedimentary environments of the northwestern Weddell Sea and South Sandwich Islands, Antarctica. Deep-Sea Research Part II 51, 1489-1514.

Hydrographic Office, 1989. South Sandwich Islands, Chart No. 3593 (1994 edition), 1:500 000, Admiralty Hydrographic Department, Taunton.

Iizasa, K., Fiske, R.S., Ishizuka, O., Yuasa, M., Hashimoto, J., Ishibashi, J., Naka, J., Horii, Y., Imail, A., Koyama, S., 1999. A Kuroko-type polymetallic sulphide deposit in a submarine silicic caldera. Science 283, 975-977.

Keating, B.H., Helsley, C.E., Karogodina, I., 2000. Sonar studies of submarine mass wasting and volcanic structures off Savaii Island, Samoa. Pure and Applied Geophysics 157, 1285-1313.

Kokelaar, P., 1986. Magma-water interactions in subaqueous and emergent basaltic volcanism. Bulletin of Volcanology 48, 275-289.

Lachlan-Cope, T., Smellie, J.L., Ladkin, R. 2001. Discovery of a recurrent lava lake on Saunders Island (South Sandwich Islands) using AVHRR imagery. Journal of Volcanology and Geothermal Research 112, 105-116.

Larter, R.D., King, E.C., Leat, P.T., Reading, A.M., Smellie, J.L., Smythe, D.K., 1998. South Sandwich slices reveal much about arc structure, geodynamics and composition. Eos, Transactions of the American Geophysical Union 79(24), 281-285.

Larter, R.D., Vanneste, L.E., Morris, P., Smyth, D.K., 2003. Structure and Tectonic evolution of the South Sandwich arc, in: Larter, R.D., Leat, P.T. (Eds.), Intra-Oceanic Subduction Systems: Tectonic and Magmatic Processes. Geological Society, London, Special Publications 219, pp. 255-284.

Leat, P.T., Smellie, J.L., Millar, I.L., Larter, R.D., 2003. Magmatism in the South Sandwich arc, in: Larter, R.D., Leat, P.T. (Eds.), Intra-Oceanic Subduction Systems: Tectonic and Magmatic Processes. Geological Society, London, Special Publications 219, pp. 285-313.

Leat, P.T., Pearce, J.A., Barker, P.F., Millar, I.L., Barry T.L., Larter, R.D., 2004. Magma genesis and mantle flow at a subducting slab edge: the South Sandwich arc-basin system. Earth and Planetary Science Letters 227, 17-35.

Leat, P.T., Larter R.D., Millar I.L., 2007. Silicic magmas of Protector Shoal, South Sandwich arc: indicators of generation of primitive continental crust in an island arc. Geological Magazine 144, 179-190.

Lee, H.J., Syvitski, J.P.M., Parker, G., Orange, D., Locat, J., Hutton, E.W.H., Imran, J., 2002. Distinguishing sediment waves from slope failure deposits: field examples, including the ‘Humboldt slide’ and modelling results. Marine Geology 192, 79-104.

Le Friant, A., Harford, C.L., Deplus, C., Boudon, G., Sparks, R.S.J., Herd R.A., Komorowski, J.C., 2004. Geomorphological evolution of Montserrat (West Indies): importance of flank collapse and erosional processes. Journal of the Geological Society, London 161, 147-160.

Lipman, P.W., Normark, W.R., Moore, J.G., Wilson J.B., Gutmacher, C.E., 1988. The giant submarine Alika debris slide, Mauna Loa, Hawaii. Journal of Geophysical Research 93, 4279-4299.

Livermore, R., 2003. Back-arc spreading and mantle flow in the East Scotia Sea, in: Larter, R.D., Leat, P.T. (Eds.), Intra-Oceanic Subduction Systems: Tectonic and Magmatic Processes. Geological Society, London, Special Publications 219, pp. 315-331.

Livermore, R., Cunningham, A., Vanneste, L., Larter R., 1997. Subduction influence on magma supply at the East Scotia Ridge. Earth and Planetary Science Letters 150, 261-275.

Longton, R.E., Holdgate, M.W., 1979. South Sandwich Islands: IV. Botany, British Antarctic Survey Scientific Reports 94.

Maldonado, A., Barnolas, A., Bohoyo, F., Galindo-Zaldívar, J., Hernández-Molina, J., Lobo, F., Rodríguez-Fernández, J., Somoza, L., Vázquez, J.T., 2003. Contourite deposits in the central Scotia Sea: the importance of the Antarctic circumpolar current and the Weddell gyre flows. Palaeogeography Palaeoclimatology Palaeoecology 198, 187-221.

Massoth, G., Baker, E., Worthington, T., Lupton, J., de Ronde, C., Arculus, R., Walker, S., Nakamura, K., Ishibashi, J., Stoffers, P., Resing, J., Greene R., Lebon, G., 2007. Multiple hydrothermal sources along the south Tonga arc and Valu Fa

Ridge. Geochemistry Geophysics Geosystems 8, Q11008, doi:10.1029/2007GC001675.

Migeon, S., Savoye, B., Faugeres J.-C., 2000. Quaternary development of migrating sediment waves in the Var deep-sea fan: distribution, growth pattern, and implication for levee evolution. Sedimentary Geology 133, 265-293.

Mitchell, N.C., Masson, D.G., Watts, A.B., Gee, M.J.R., Urgeles, R., 2002. The morphology of the submarine flanks of volcanic ocean islands. A comparative study of the Canary and Hawaii hotspot islands. Journal of Volcanology and Geothermal Research 115, 83-107.

Normark, W.R., Piper, D.J.W., Posamentier, H., Pirmez, C., Migeon, S., 2002. Variability in form and growth of sediment waves on turbidity channel levees. Marine Geology 192, 23-58.

Oakley, A.J., Taylor, B., Moore, G.F., Goodliffe, A., 2009. Sedimentary, volcanic, and tectonic processes of the central Mariana arc: Mariana back-arc basin formation and the West Marina Ridge. Geochemistry Geophysics Geosystems 10, Q08X07, doi:10.1029/2008GC002312.

Patrick, M.R., Smellie, J.L., Harris, A.J.L., Wright, R., Dean, K., Izbekov, P., Garbeil, H., Pilger, E., 2005. First recorded eruption of Mount Belinda volcano (Montagu Island, South Sandwich Islands). Bulletin of Volcanology 67, 415-422.

Pearce, J.A., Baker, P.E., Harvey, P.K., Luff, I.W., 1995. Geochemical evidence for subduction fluxes, mantle melting and fractional crystallization beneath the South Sandwich arc. Journal of Petrology 36, 1073-1109.

Pudsey, C.J., 2002. The Weddell Sea: contourites and hemipelagites at the northern margin of the Weddell Gyre, in: Stow, D.A.V., Pudsey, C.J., Howe, J.A., Faugères, J.-C., Viana, A.R. (Eds.), Deep-Water Contourite Systems: Modern

Drifts and Ancient Series, Seismic and Sedimentary Characteristics. Geological Society, London, Memoirs 22, pp. 289-303.

Risso, C., Scasso, R.A., Aparicio, A., 2002. Presence of large pumice blocks on Tierra del Fuego and South Shetland Islands shorelines, from 1962 South Sandwich Islands eruption. Marine Geology 186, 413-422.

Romagnoli, C., Kokelaar, P., Casalbore, D., Chiocci, F.L., 2009. Lateral collapses and active sedimentary processes on the northwestern flank of Stromboli volcano, Italy. Marine Geology 265, 101-119.

Satake, K., Kato, Y., 2001. The 1741 Oshima-Oshima eruption: extent and volume of submarine debris avalanche. Geophysical Research Letters 28, 427-430.

Siebert, L., 1984. Large volcanic debris avalanches: characteristics of source areas, deposits, and associated eruptions. Journal of Volcanology and Geothermal Research 22, 163-197.

Siebert, L., Glicken, H., Ui, T., 1987. Volcanic hazards from Bezymianny- and Bandai-type eruptions. Bulletin of Volcanology 49, 435-459.

Silver, E., Day, S., Ward, S., Hoffmann, G., Llanes, P., Lyons, A., Driscoll, N., Prembo, R., John, S., Saunders, S., Taranu, F., Anton, L., Abiari, I., Applegate, B., Engels, J., Smith, J., Tagliodes T., 2005. Island arc debris avalanches and tsunami generation. Eos, Transactions of the American Geophysical Union 86(47), 485, 489.

Silver, E., Day, S., Ward, S., Hoffmann, G., Llanes, P., Driscoll, N., Appelgate, B., Saunders, S., 2009. Volcano collapse and tsunami generation in the Bismarck Volcanic Arc, Papua New Guinea. Journal of Volcanology and Geothermal Research 186, 210-222.

Smellie, J.L., Morris, P., Leat, P.T. Turner, D.B. Houghton, D., 1998. Submarine caldera and other volcanic observations in Southern Thule, South Sandwich Islands. Antarctic Science 10, 171-172.

Stüben, D., Bloomer, S.H., Taïbi, N.E., Neumann, T., Bendel, V., Püschel, U., Barone, A., Lange, A., Shiying, W., Cuizhong, L., Deyu, Z., 1992. First results of study of sulphur-rich hydrothermal activity from an island-arc environment: Esmeralda Bank in the Mariana arc. Marine Geology 103, 521-528.

Tani, K., Fiske, R.S., Tamura, Y., Kido, Y., Naka, J., Shukuno, H., Takeuchi, R., 2008. Sumisu volcano, Izu-Bonin arc, Japan: site of a silicic caldera-forming eruption from a small open-ocean island. Bulletin of Volcanology 70, 547-562.

Tappin, D.R., Watts, P., McMurtry, G.M., Lafoy, Y., Matsumoto, T., 2001. The Sissano Papua New Guinea tsunami of July 1998 – offshore evidence on the source mechanism. Marine Geology 175, 1-23.

Tate, A.J., Leat P.T., 2007. RRS James Clark Ross JR168 cruise report: swath bathymetry South Sandwich Islands. British Antarctic Survey Report ES6/1/2007/1, https://www.bodc.ac.uk/data/information_and_inventories/cruise_inventory/report/9079/

Thomas, C., Livermore, R.A., Pollitz, F.F., 2003. Motion of the Scotia Sea plates. Geophysical Journal International 155, 789-804.

Tomblin, J.F., 1979. The South Sandwich Islands: II. The Geology of Candlemas Island. British Antarctic Survey Science Reports 92.

Vanneste, L.E., Larter, R.D., 2002. Sediment subduction, subduction erosion, and strain regime in the northern South Sandwich forearc. Journal of Geophysical Research 107(B7), 2149, doi:10.1029/2001JB000396.

Vanneste, L.E., Larter, R.D., Smyth, D.K., 2002. Slice of intraoceanic arc: insights from the first multichannel seismic reflection profile across the South Sandwich island arc. Geology 30, 819-822.

Wright, I.C., Worthington, T.J., Gamble, J.A., 2006. New multibeam mapping and geochemistry of the 30º-35ºS sector, and overview, of southern Kermadec arc volcanism. Journal of Volcanology and Geothermal Research 149, 263-296.

Wynn, R.B., Masson, D.G., Stow, D.A.V., Weaver P.P.E., 2000. Turbidity current sediment waves on the submarine slopes of the western Canary Islands. Marine Geology 163, 185-198.

Wynn, R.B., Piper, D.J.W., Gee, M.R., 2002. Generation and migration of course-grained sediment waves in turbidity current channels and channel-lobe transition zones. Marine Geology 192, 59-78.

Figure captions

Fig. 1. A. Regional setting of the South Sandwich arc in the South Atlantic. B. Location of the survey area within the South Sandwich arc. The South American plate is subducting beneath the Sandwich plate, which is diverging from the Scotia Plate at the East Scotia Ridge spreading center. The new survey area is within the dashed line, and the previous MR1 survey (Vanneste and Larter, 2002; Livermore, 2003) is also shown. E1-E10 are segments of the spreading center, and main volcanoes of the arc are: P, Protector Shoal; Z, Zavodovski; L, Leskov; V, Visokoi; C-V, Candlemas-

Vindication; S, Saunders; M, Montagu; B, Bristol; ST, Southern Thule; K, Kemp seamount, N, Nelson seamount. Arrows show relative plate motions.

Fig. 2 Map of the northern South Sandwich arc showing the new bathymetric data. A. topography. B. derived slopes. Projection: Mercator. Sections A-A', B-B' and C-C' are shown in Fig. 12. P, Protector Shoal; Z, Zavodovski; V, Visokoi; C-V, Candlemas-Vindication.

Fig. 3. Bathymetric map of the Protector Shoal area from the new multibeam data. Features PS1 to PS7 are seamounts. The location of dredge DR.162 is shown. Faults downthrow to the southeast. Black arrows indicate movement in slumps and chutes; white arrows indicate currents depositing sediment waves.

Fig. 4. A. Detail of the interpreted slump on the southern flank of seamount PS4. B. Detail of the caldera on seamount PS7.

Fig. 5. TOPAS profiles of slumps on seamount PS4, locations of lines shown in Fig. 3. A. Line JR206_23a. B. Line JR206_24. C. Section of JR206_25. All data are plotted with 5 x vertical exaggeration and vertical axes are ms TWTT.

Fig. 6. Map of the area around Zavodovski Island from the new multibeam data. Positive features ZE1-3, ZW1-6 and hills H1-2 are described in the text.

Fig. 7. Photographs and details of Zavodovski volcano. A. View of Zavodovski Island from the west, with the active crater largely obscured by cloud. The older collapse

headwall is part of the Mount Curry collapse. The embayment caused by this event exposes horizontal pre-collapse lavas in the sea cliffs. The embayment is partly filled by recent scoria from the active crater. B. Zavodovski Island viewed from the north. An inactive crater rim is picked out by the upper limit of gullies in the scoria. This crater was probably filled by scoria from the active crater, which is beyond the visible summit. Lavas form a delta and ca. 10 m high cliffs. C. Detail of Zavodovski volcano, showing the Mount Curry landslide in the foreground. D. View of Zavodovski volcano from the east, showing sediment wave field in the foreground.

Fig. 8. Sample data from JR206 TOPAS lines 27 and 29 from the sediment wave field east of Zavodovski, locations shown in Fig. 6. Seabed plots of complete lines plotted at 5 x vertical exaggeration, magnified figures A – E plotted with 10 x vertical exaggeration. Basic interpretation shown: seabed, stratified sediments, inferred deeper reflector and boundary between stratified and more compacted sediments represented by blue, yellow, green and red respectively. All vertical axes are ms TWTT.

Fig. 9. Photographs and details of Visokoi volcano. A. Visokoi Island viewed from the southwest. The summit is covered by an ice sheet, and the steep slopes west of the summit are visible. B. Mafic dikes cutting scoria, south coast of Visokoi Island. Note figure for scale. C. South west flank of Visokoi showing rugged topography interpreted as formed by eruption of lava domes or cones; landslide chutes are directed toward the bottom left of the image.

Fig. 10. Map of the area around Visokoi, and the Candlemas group from the new multibeam data. Ridges CA1-5, embayments ECE1-2, SCE, WCE and NCE, and hill H3 are described in the text.

Fig. 11. A. Sketch of the Candlemas-Vindication area, showing the approximate area covered by the shallow shelf, as defined by the 100 m contour (Hydrographic Office, 1989; this survey), and the position of eroded sea stacks forming small islands. The direction of view of photographs B-E are shown by arrows. B. Candlemas Island viewed from the southeast. Mounts Andromeda and Perseus consist of eroded basaltic lavas. Note the ice sheet between the two summits. C. Vindication Island viewed from the southeast. The sea cliffs expose interbedded basaltic lavas and scoria. Cook Rock is the largest of several small islands and shoals between Vindication and Candlemas islands. D. The northern, recent part of Candlemas Island, viewed from the east. Lucifer Hill is a recent volcano, surrounded by andesite and dacite blocky lava deltas. The boulder beach joins the lavas to the northern slope of Mount Perseus, which forms the foreground and isolates Gorgon Pool from the ocean. The boulder beach and foreground is populated by a large colony of penguins. E. The western flank of Lucifer Hill, looking southwest toward Vindication Island and Cook Rock. Fumarolically altered scoria and lava form the foreground. The blocky lava flow is andesitic and has concentric pressure ridges.

Fig. 12. Approximately east-west bathymetric profiles across Zavodovski, Visokoi and Candlemas volcanoes. Vertical exaggeration x 5. Locations of A-A', B-B' and C-C' are shown in Fig. 2.

Table 1. Summary of features of seamounts in the Protector Shoal seamount chain

Seamount	Summit latitude	Summit longitude	Height m	Shallowest point below s.l. m	Basal contour m	Basal diameter km	Estimated volume (km^3)	Flank slopes°	Features
PS1	55°55.5'S	27°42.1'W	425	275	700	9	9	1.9-8.1	Smooth outline
PS2	55°57.0'S	27°51.4'W	757	243	1000	9	16	3.6-13.9	Smooth outline
PS3	55°56.6'S	27°58.1'W	432	568	1000	6	4	2.4-8.4	Smooth outline
PS4	55°56.3'S	28°6.0'W	845	55	900	14	43	1.0-11.3	Identified as Protector Shoal. Major slump scar on S flank. Slump on NW flank
PS5	56°0.8'S	28°15.1'W	1260	440	1700	13	55	4.6-16.9	Satellite domes
PS6	55°54.8'S	28°24.8'W	1418	82	1500	15	83	5.1-17.6	Slide scar on SW flank
PS7	55°49.5'S	28°30.2'W	646	654	1300	10	16	6.2-13.7	3 km nested caldera

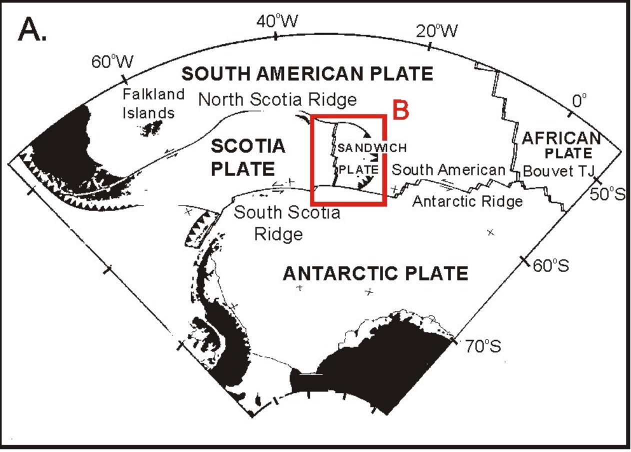
A.
40°W
20°W
60°W
SOUTH AMERICAN PLATE
Falkland Islands
North Scotia Ridge
B
0°
SCOTIA PLATE
SANDWICH PLATE
AFRICAN PLATE
South American
Bouvet TJ
50°S
Antarctic Ridge
South Scotia Ridge
60°S
ANTARCTIC PLATE
70°S

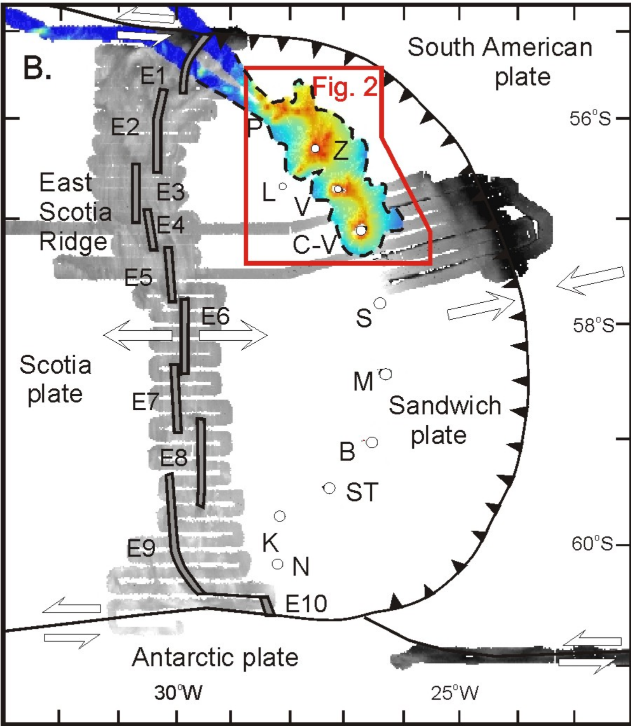
B.
South American plate
Fig. 2
E1
E2
P
56°S
Z
East Scotia Ridge
E3
L
V
E4
C-V
E5
E6
S
58°S
Scotia plate
M
Sandwich plate
E7
B
E8
ST
K
60°S
E9
N
E10
Antarctic plate
30°W
25°W

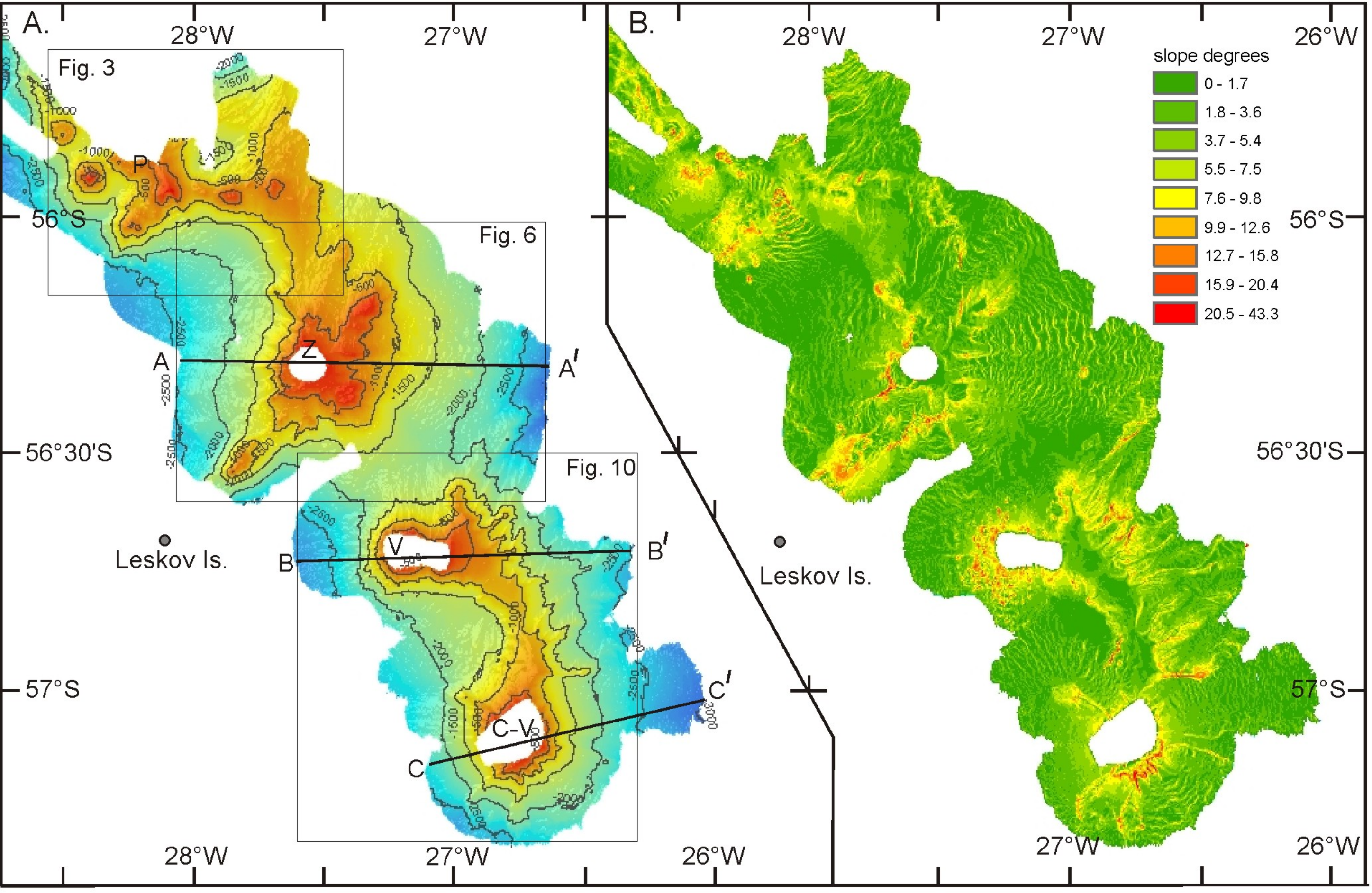

A.
B.
28°W
27°W
26°W
56°S
56°30'S
57°S
Fig. 3
Fig. 6
Fig. 10
P
Z
V
C-V
A
A'
B
B'
C
C'
Leskov Is.
slope degrees
0 - 1.7
1.8 - 3.6
3.7 - 5.4
5.5 - 7.5
7.6 - 9.8
9.9 - 12.6
12.7 - 15.8
15.9 - 20.4
20.5 - 43.3

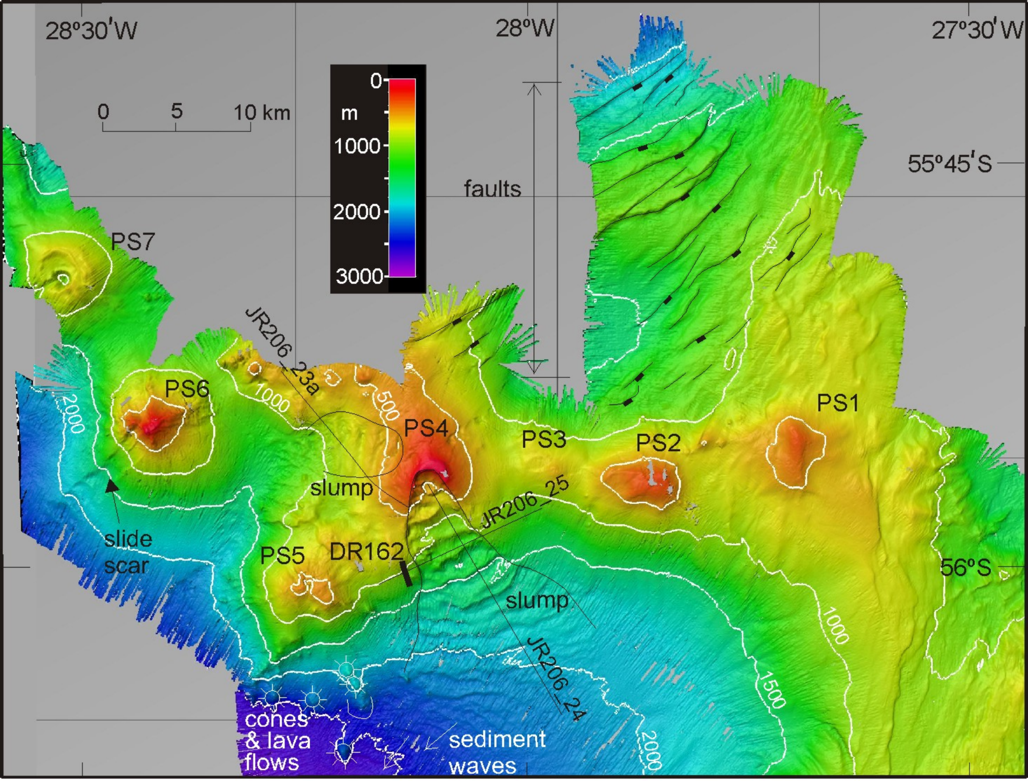
28°30′W
28°W
27°30′W
0
5
10 km
0
m
1000
2000
3000
faults
55°45′S
56°S
PS7
PS6
PS5
PS4
PS3
PS2
PS1
JR206_23a
JR206_25
JR206_24
DR162
1000
500
2000
1500
slump
slump
slide
scar
cones
& lava
flows
sediment
waves

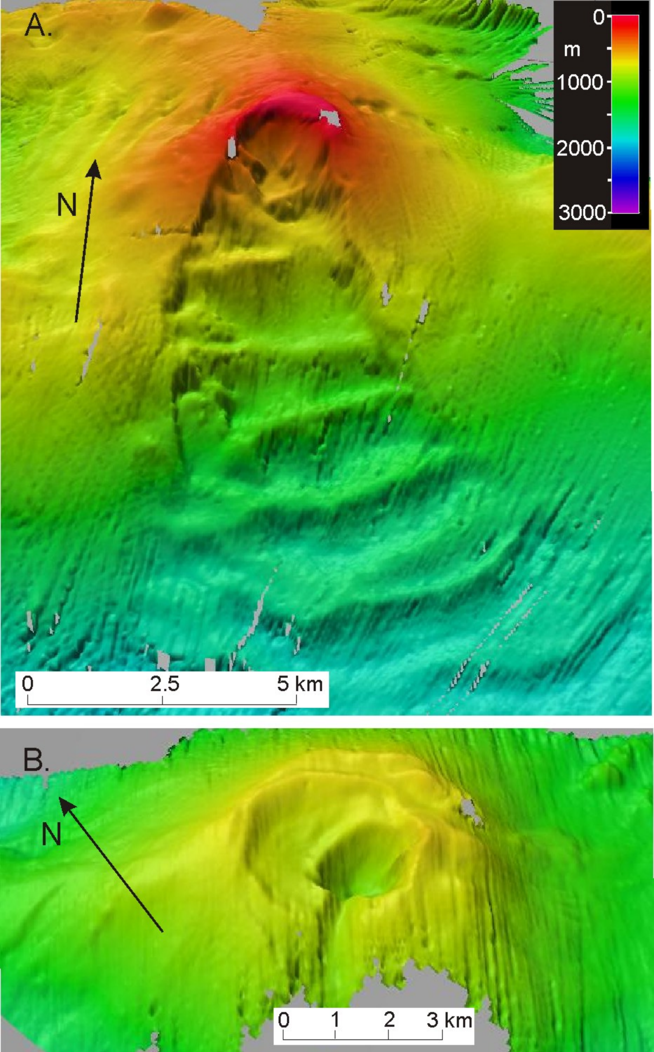
A.
0
m
1000
2000
3000
N
0
2.5
5 km
B.
N
0
1
2
3 km

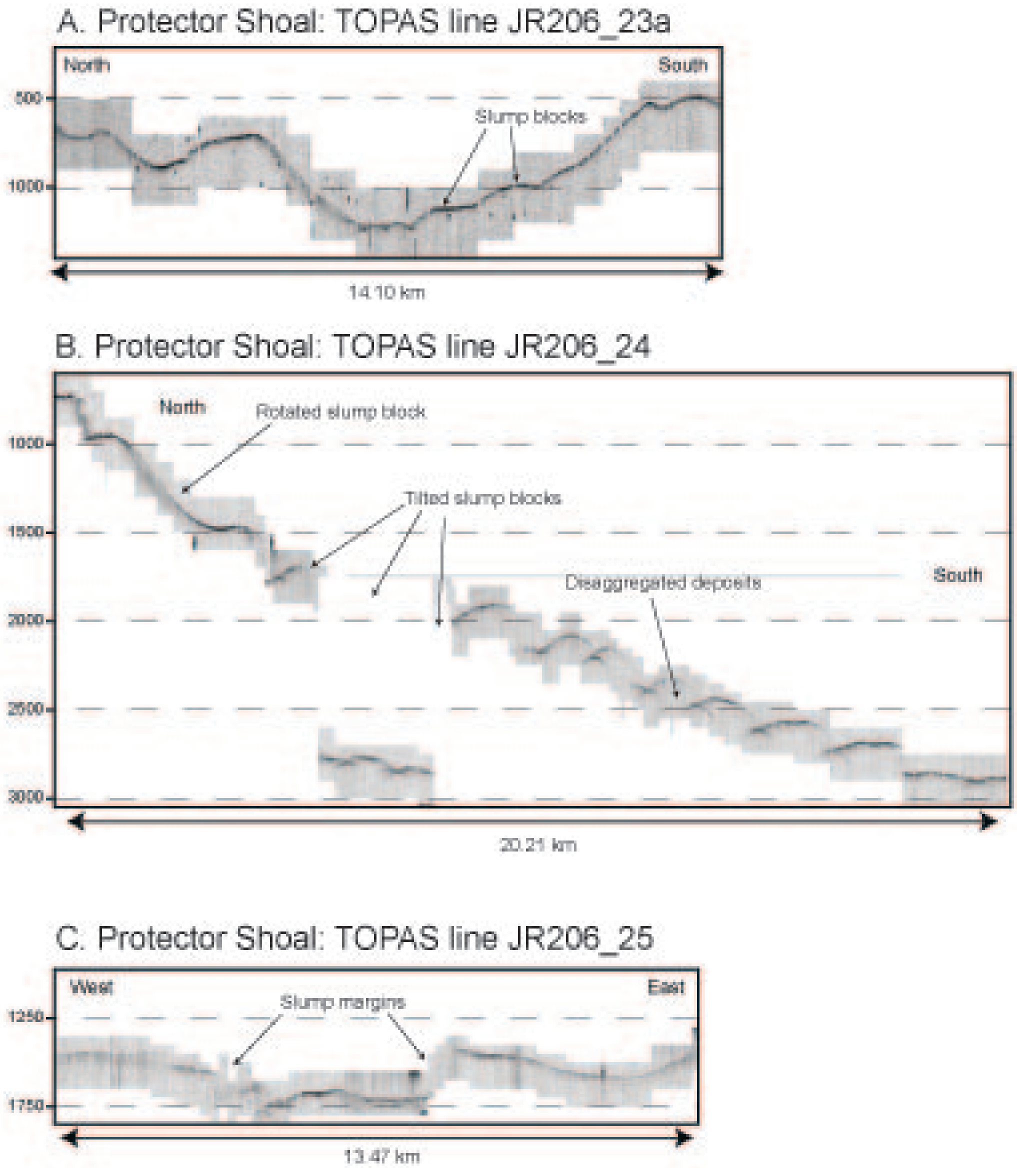
A. Protector Shoal: TOPAS line JR206_23a
North
South
Slump blocks
500
1000
14.10 km
B. Protector Shoal: TOPAS line JR206_24
North
Rotated slump block
Tilted slump blocks
Disaggregated deposits
South
1000
1500
2000
2500
3000
20.21 km
C. Protector Shoal: TOPAS line JR206_25
West
East
Slump margins
1250
1750
13.47 km

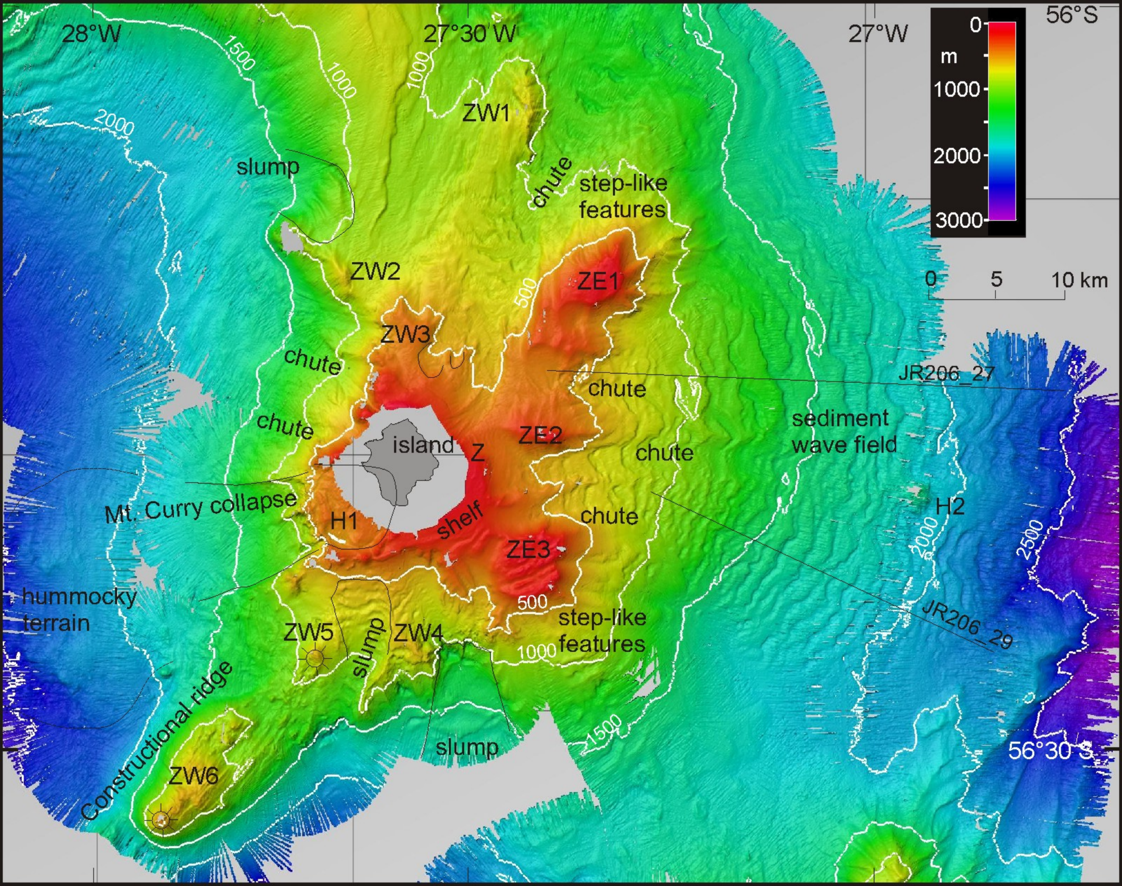
28°W
27°30'W
27°W
56°S
56°30'S
m
0
1000
2000
3000
0 5 10 km
500
1000
1500
2000
2500
ZW1
ZW2
ZW3
ZW4
ZW5
ZW6
ZE1
ZE2
ZE3
H1
H2
Z
island
shelf
slump
chute
step-like features
sediment wave field
Mt. Curry collapse
hummocky terrain
Constructional ridge
JR206_27
JR206_29

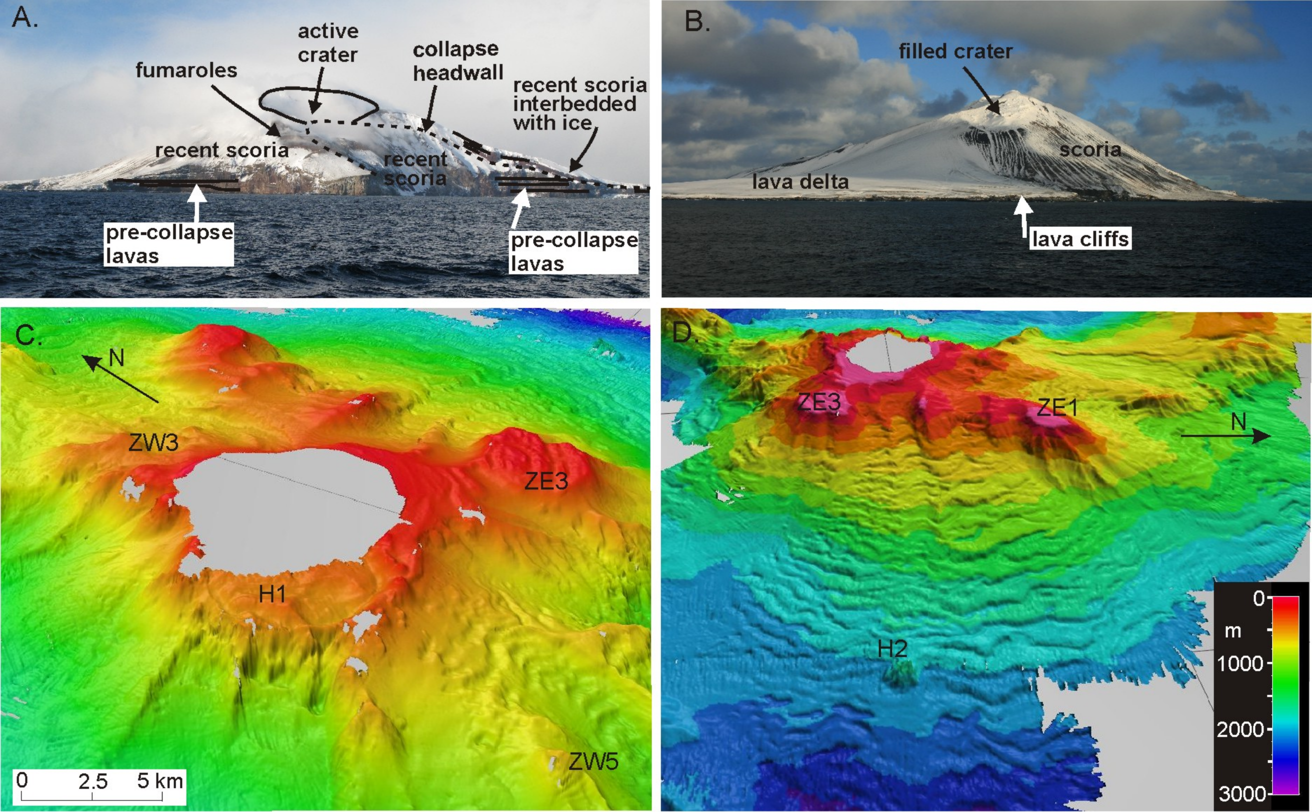
A.
active
crater
fumaroles
collapse
headwall
recent scoria
interbedded
with ice
recent scoria
recent
scoria
pre-collapse
lavas
pre-collapse
lavas
B.
filled crater
scoria
lava delta
lava cliffs
C.
N
ZW3
ZE3
H1
ZW5
0
2.5
5 km
D.
ZE3
ZE1
N
H2
0
m
1000
2000
3000

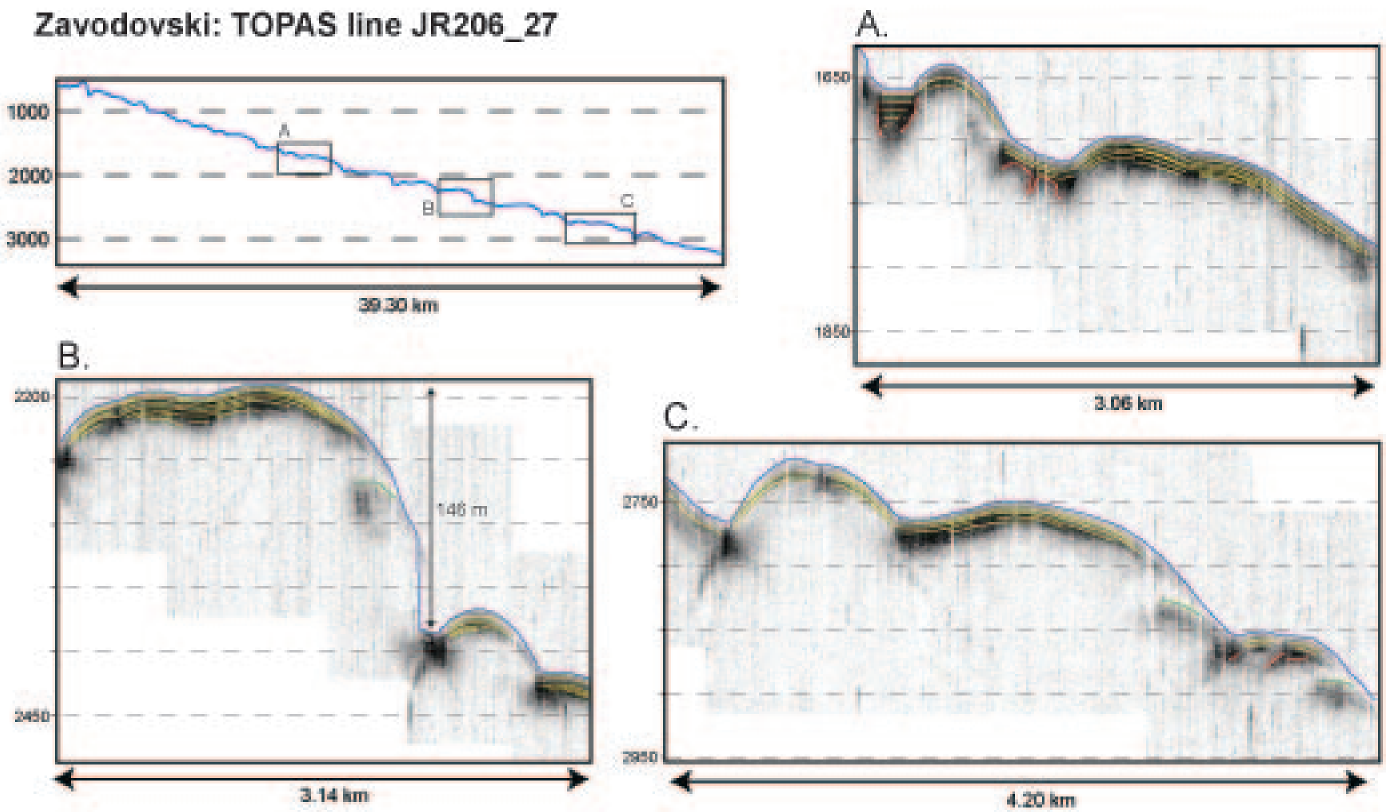
Zavodovski: TOPAS line JR206_27
1000
2000
3000
A
B
C
39.30 km
A.
1650
1850
3.06 km
B.
2200
146 m
2450
3.14 km
C.
2750
2950
4.20 km

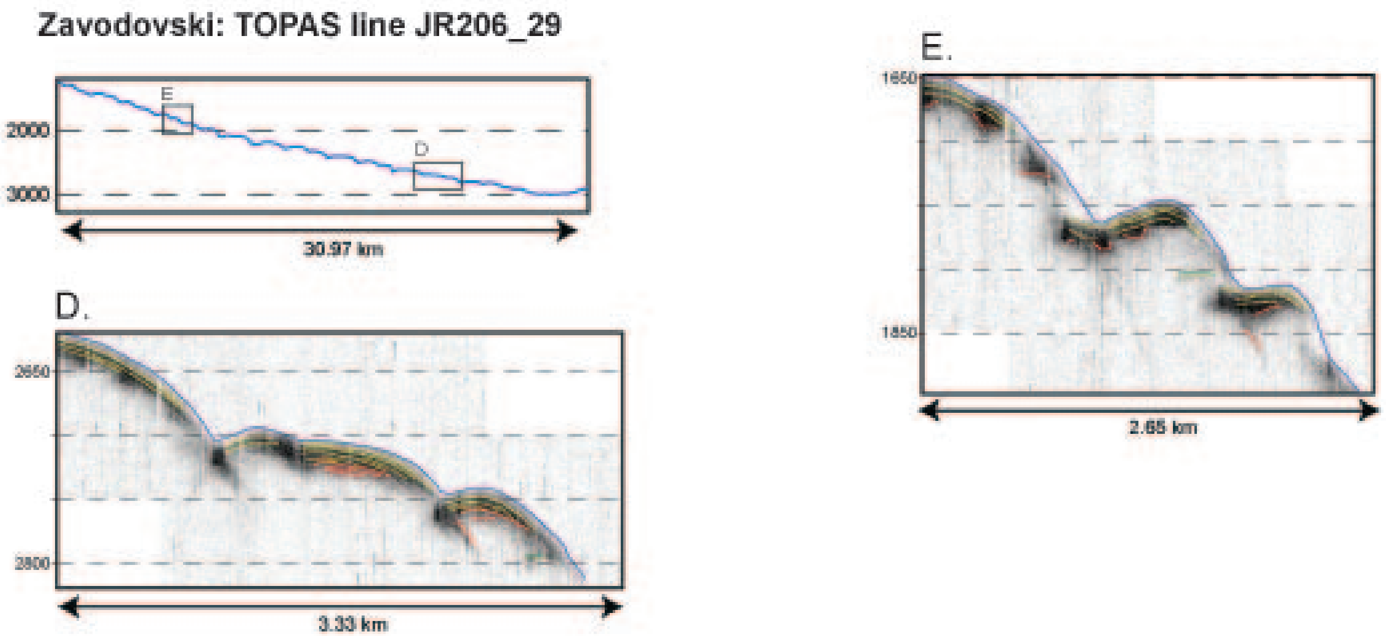
Zavodovski: TOPAS line JR206_29
2000
3000
E
D
30.97 km
E.
1650
1850
2.65 km
D.
2650
2800
3.33 km

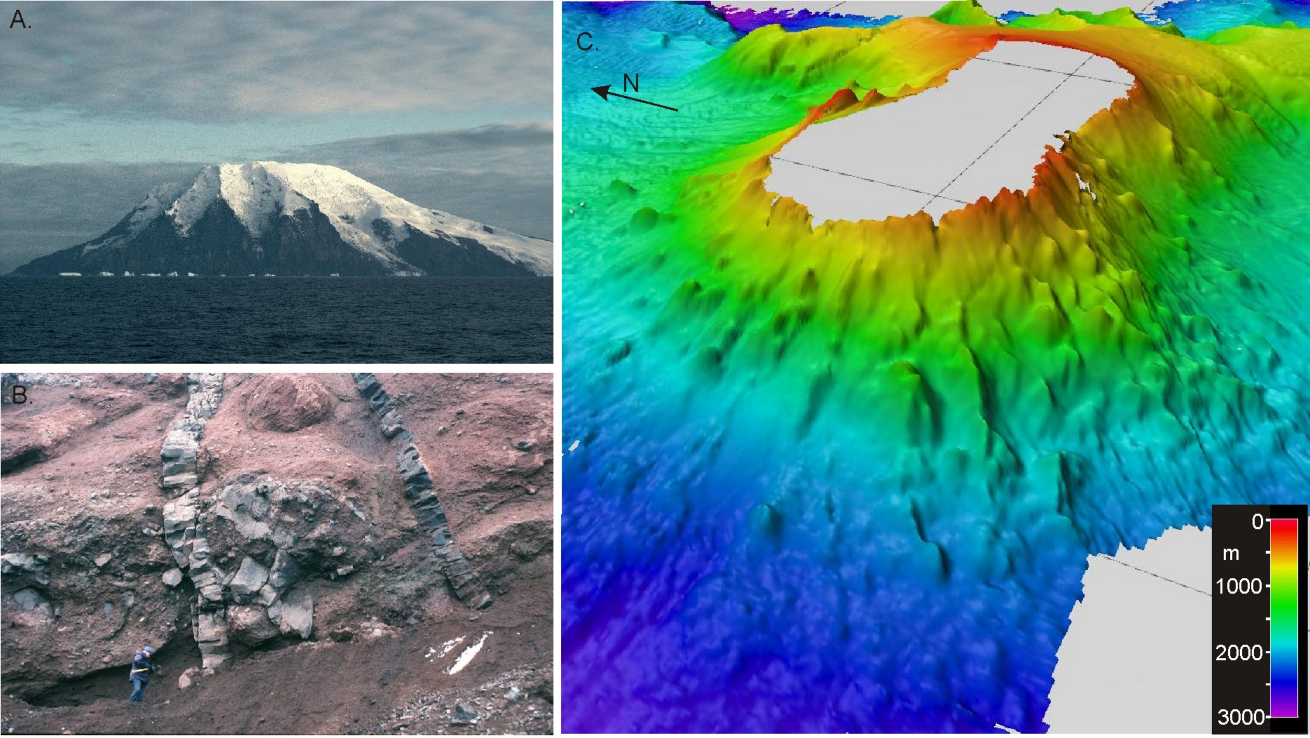
A.
B.
C.
N
0
m
1000
2000
3000

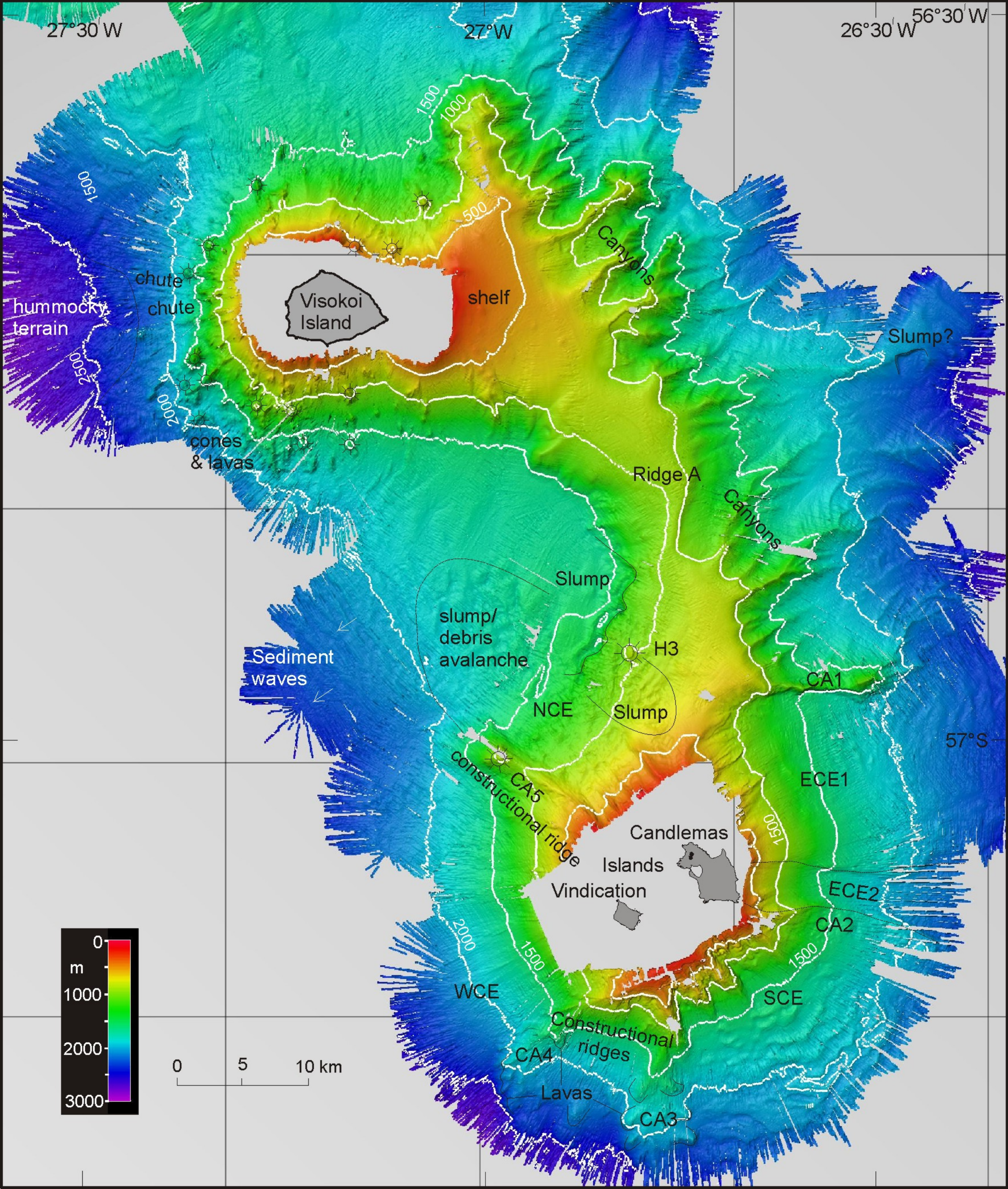

27°30'W
27°W
26°30'W
56°30'W
1500
1000
500
1500
2500
2000
hummocky terrain
chute
chute
Visokoi Island
shelf
Canyons
Slump?
cones & lavas
Ridge A
Canyons
Slump
slump/ debris avalanche
Sediment waves
H3
CA1
NCE
Slump
57°S
CA5
constructional ridge
ECE1
1500
Candlemas
Islands
Vindication
ECE2
CA2
2000
1500
1500
WCE
SCE
Constructional ridges
CA4
Lavas
CA3
0
m
1000
2000
3000
0
5
10 km

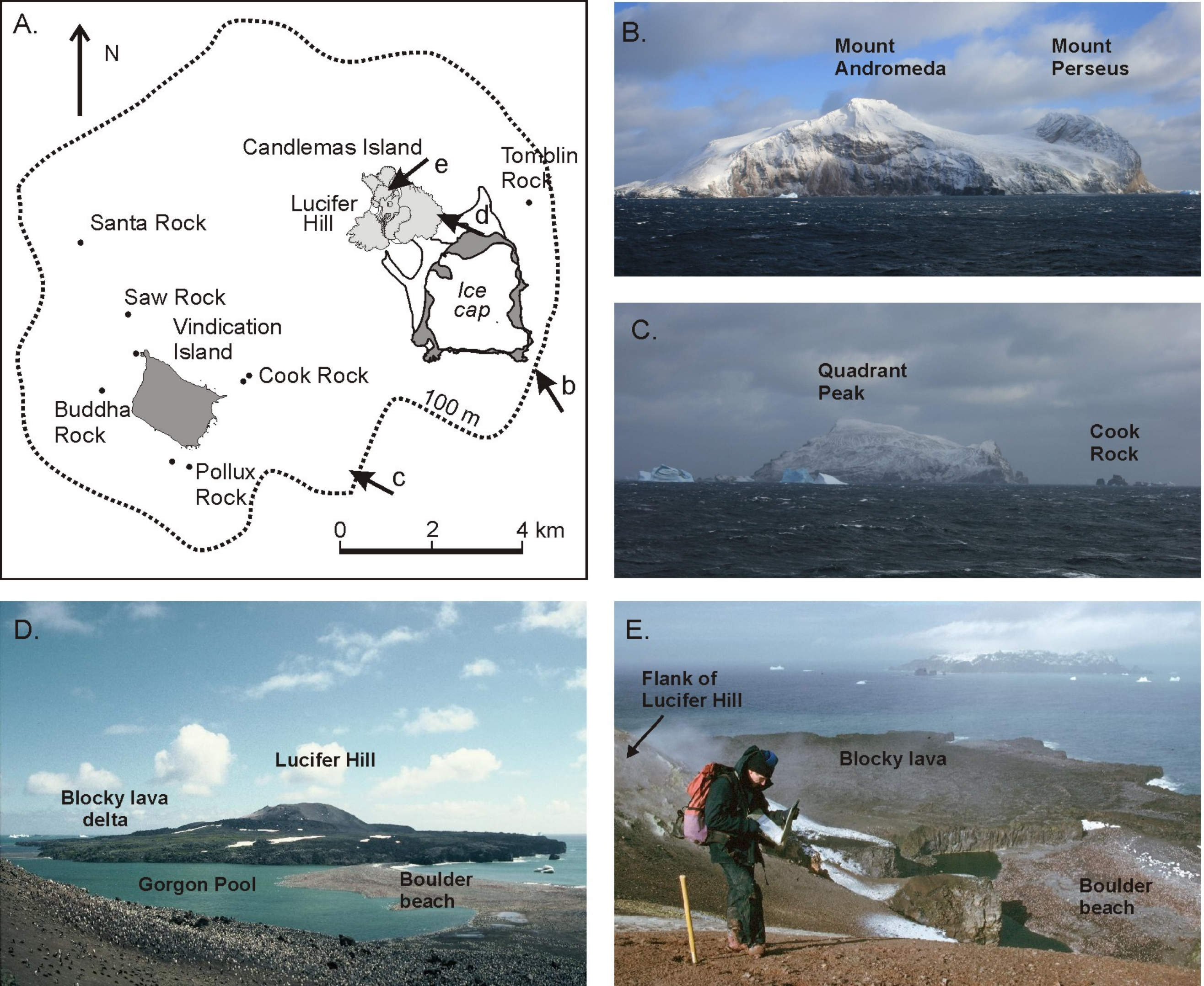

A.
N
Candlemas Island
e
Tomblin Rock
Lucifer Hill
d
Santa Rock
Ice cap
Saw Rock
Vindication Island
Cook Rock
b
Buddha Rock
100 m
Pollux Rock
c
0
2
4 km
B.
Mount Andromeda
Mount Perseus
C.
Quadrant Peak
Cook Rock
D.
Lucifer Hill
Blocky lava delta
Gorgon Pool
Boulder beach
E.
Flank of Lucifer Hill
Blocky lava
Boulder beach

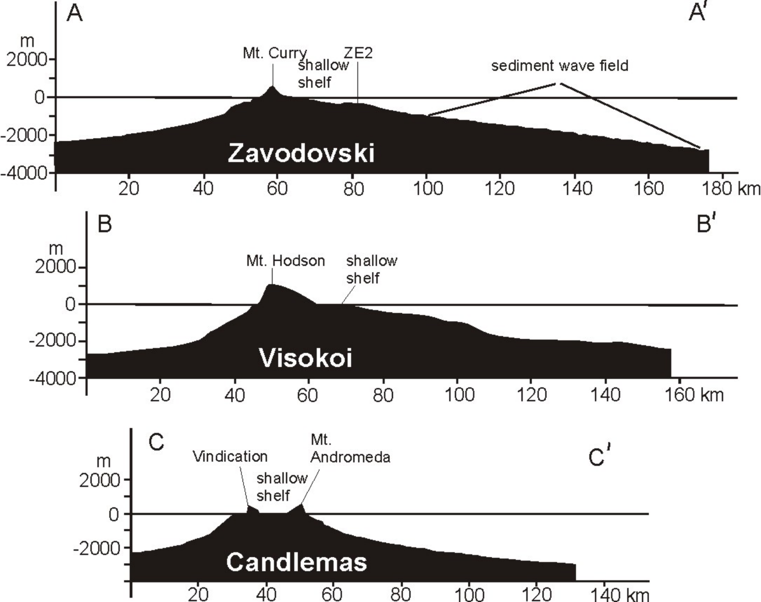

A
A'
m
2000
0
-2000
-4000
Mt. Curry
shallow shelf
ZE2
sediment wave field
Zavodovski
20
40
60
80
100
120
140
160
180 km
B
B'
m
2000
0
-2000
-4000
Mt. Hodson
shallow shelf
Visokoi
20
40
60
80
100
120
140
160 km
C
C'
m
2000
0
-2000
Vindication
Mt. Andromeda
shallow shelf
Candlemas
20
40
60
80
100
120
140 km